NAVAL POSTGRADUATE SCHOOL

MONTEREY, CALIFORNIA

THESIS

MODELING AND SIMULATION OF THE FREE ELECTRON LASER AND RAILGUN ON AN ELECTRIC NAVAL SURFACE PLATFORM

by

Oscar E. Bowlin

March 2006

Thesis Advisor: William B. Colson
Second Reader: Robert L. Armstead

Approved for public release; distribution is unlimited

THIS PAGE INTENTIONALLY LEFT BLANK

REPORT DOCUMENTATION PAGE			Form Approved OMB No. 0704-0188
Public reporting burden for this collection of information is estimated to average 1 hour per response, including the time for reviewing instruction, searching existing data sources, gathering and maintaining the data needed, and completing and reviewing the collection of information. Send comments regarding this burden estimate or any other aspect of this collection of information, including suggestions for reducing this burden, to Washington headquarters Services, Directorate for Information Operations and Reports, 1215 Jefferson Davis Highway, Suite 1204, Arlington, VA 22202-4302, and to the Office of Management and Budget, Paperwork Reduction Project (0704-0188) Washington DC 20503.			
1. AGENCY USE ONLY ***(Leave blank)***	**2. REPORT DATE** March 2006	**3. REPORT TYPE AND DATES COVERED** Master's Thesis	
4. TITLE AND SUBTITLE: Modeling and Simulation of the Free Electron Laser and Railgun on an Electric Naval Surface Platform		**5. FUNDING NUMBERS**	
6. AUTHOR(S) Bowlin, Oscar E.			
7. PERFORMING ORGANIZATION NAME(S) AND ADDRESS(ES) Naval Postgraduate School Monterey, CA 93943-5000		**8. PERFORMING ORGANIZATION REPORT NUMBER**	
9. SPONSORING /MONITORING AGENCY NAME(S) AND ADDRESS(ES) N/A		**10. SPONSORING/MONITORING AGENCY REPORT NUMBER**	
11. SUPPLEMENTARY NOTES The views expressed in this thesis are those of the author and do not reflect the official policy or position of the Department of Defense or the U.S. Government.			
12a. DISTRIBUTION / AVAILABILITY STATEMENT Approved for public release; distribution is unlimited		**12b. DISTRIBUTION CODE**	
13. ABSTRACT (maximum 200 words) The Free Electron Laser (FEL) and Rail Gun are electric weapons which will require a significant amount of stored energy for operation. These types of weapons are ideal for use onboard an all-electric ship. An investigation is made of the effects these weapons will have on a proposed electrical system architecture using simulation modeling. Specifically, this thesis identifies possible design weaknesses and shows where further research and modeling is needed in order to ensure the proper integration of these electric weapons onboard an all-electric ship. The integration of these electric weapon systems with the power systems on electric ships will have an impact on naval operations. Several scenarios concerning specific naval missions are investigated using simulation software to understand the impact and limitations on the electric system using these new electric weapons.			
14. SUBJECT TERMS Free Electron Laser, FEL, Railgun, Simulink, Directed Energy, Flywheels, Capacitors, SMES, Batteries, Integrated Propulsion System, AMFRC			**15. NUMBER OF PAGES** 75
			16. PRICE CODE
17. SECURITY CLASSIFICATION OF REPORT Unclassified	**18. SECURITY CLASSIFICATION OF THIS PAGE** Unclassified	**19. SECURITY CLASSIFICATION OF ABSTRACT** Unclassified	**20. LIMITATION OF ABSTRACT** UL

NSN 7540-01-280-5500 Standard Form 298 (Rev. 2-89)
Prescribed by ANSI Std. 239-18

THIS PAGE INTENTIONALLY LEFT BLANK

Approved for public release; distribution is unlimited

MODELING AND SIMULATION OF THE FREE ELECTRON LASER AND RAILGUN ON AN ELECTRIC NAVAL SURFACE PLATFORM

Oscar E. Bowlin
Lieutenant, United States Navy
B.S., Old Dominion University, 1998

Submitted in partial fulfillment of the
requirements for the degree of

MASTER OF SCIENCE IN APPLIED PHYSICS

from the

NAVAL POSTGRADUATE SCHOOL
March 2006

Author: Oscar E. Bowlin

Approved by: William B. Colson
Thesis Advisor

Robert L. Armstead
Second Reader

James H. Luscombe
Chairman, Department of Physics

THIS PAGE INTENTIONALLY LEFT BLANK

ABSTRACT

The Free Electron Laser (FEL) and Rail Gun are electric weapons which will require a significant amount of stored energy for operation. These types of weapons are ideal for use onboard an all-electric ship. An investigation is made of the effects these weapons will have on a proposed electrical system architecture using simulation modeling. Specifically, this thesis identifies possible design weaknesses and shows where further research and modeling is needed in order to ensure the proper integration of these electric weapons onboard an all-electric ship. The integration of these electric weapon systems with the power systems on electric ships will have an impact on naval operations. Several scenarios concerning specific naval missions are investigated using simulation software to understand the impact and limitations on the electric system using these new electric weapons.

THIS PAGE INTENTIONALLY LEFT BLANK

TABLE OF CONTENTS

LIST OF FIGURES

LIST OF SYMBOLS

a	Dimensionless optical field
a_o	Initial dimensionless optical field
A	Capacitor plate area
$\vec{A}$	Vector potential
B	Undulator magnetic field strength
$\vec{B}$	Railgun magnetic field
$\vec{B}_1$	Magnetic field of rail 1
$\vec{B}_2$	Magnetic field of rail 2
c	Speed of light
C	Capacitance
d	Capacitor plate separation
e	Electron charge
$\vec{E}$	Electric field
$\vec{F}$	Lorentz Force
$\vec{F}_p$	Projectile force
G	Gain
k_o	Undulator wave number
K	Undulator parameter
q	Electron charge
Q	Capacitor charge
I	Current
j	Dimensionless current
$\vec{J}_\perp$	Transverse current density
L	FEL Undulator length
L	SMES Inductance
L'	Inductance gradient
m	Electron mass
N	Number of undulator periods
r	Rotor radius
R	Radius of each rail
μ_o	Permeability of free space
v_d	Electron drift velocity
V	Capacitor voltage
w	Separation distance between rails
x, y, z	Cartesian coordinates
$\vec{\beta}$	Dimensionless velocity
$\vec{\beta}_\perp$	Transverse component of $\vec{\beta}$

γ	Lorentz factor
$\hat{\varepsilon}$	Polarization unit vector
ε	Permittivity of a capacitor
ζ	Electron phase
η	Undulator extraction
λ	Optical wavelength
λ_o	Undulator period
ν	Dimensionless phase velocity
ρ_e	Electron beam density
τ	Dimensionless time
ϕ	Initial optical phase
ψ	Optical phase
ω	Optical frequency
ω_o	Undulator frequency

LIST OF ACRONYMS

AES	Advanced Energy Systems
AGT	Auxiliary Gas Turbine
AMRFC	Advanced Multifunction Radio Frequency Concept
CEM	Center for Electromechanics
CRP	Controllable Pitch Propeller
EMALS	Electromagnetic Aircraft Launch System
EML	Electromagnetic Launch
EW	Electronic Warfare
FEL	Free Electron Laser
IPS	Integrated Power System
IR	Infrared
JLAB	Jefferson National Laboratory
LCS	Littoral Combat Ship
LINAC	Linear Accelerator
MGT	Main Gas Turbine
MRG	Main Reduction Gear
NPS	Naval Postgraduate School
RCS	Radar Cross Section
RF	Radio Frequency
SMES	Superconducting Magnetic Electric Storage
SRF	Superconducting Radio Frequency
THEL	Tactical High Energy Laser

THIS PAGE INTENTIONALLY LEFT BLANK

I. INTRODUCTION

Selection of the electric drive for the United States Navy's next Destroyer (DDx), was a significant decision, and will pave the way for electric weapons onboard Navy ships. The DDx will provide a test and evaluation basis of the Integrated Power System (IPS), which may be the basic system used for the all-electric ship. The use of the IPS will provide more flexibility and much greater power availability. This power will be needed by the electric weapons of tomorrow, the Railgun and Free Electron Laser (FEL). The IPS will act as a charging device for an energy storage system(s), which will provide the properly conditioned power to the electric weapons. Each of these weapons may use their own separate energy storage devices or they could share the energy storage device. Consideration of operational scenarios with these systems is important to understand the limitations and emphasize possible weaknesses in the IPS or the consequences of sharing the energy storage.

Chapter II discusses the Integrated Power System (IPS) in regards to the propulsion and electric distribution it provides. The history of the electric drive is also discussed along with options on propulsion type that could be chosen for the electric ship.

Chapter III describes several of the possible systems that may be installed on an all-electric ship. Specifically, discussion centers on the Advanced Multifunction Radio Frequency Concept (AMRFC), the

Electromagnetic Aircraft Launch System (EMALS), the Railgun and the Free Electron Laser (FEL). The power requirements of these systems will also be considered.

Chapter IV is an in-depth discussion on the theory behind the FEL as well as some integration issues associated with installation aboard a Navy ship.

Chapter V discusses some of the pulse power equipment being considered for use as an energy storage device. Flywheels, capacitors, batteries and Superconducting Magnetic Electric Storage (SMES) are all compared and considered as viable options for use onboard Electric ships.

Chapter VI describes the Simulink® program written to simulate the electric and propulsion system of a ship. Several operational scenarios were simulated using the Railgun and FEL. Simulation results are presented and analyzed. Continued operational considerations and analysis are essential to ensuring that the design and hardware engineering of the FEL and Railgun matches the expected operational capacity. Additionally, operational expectations need to be realistic relative to available technology.

Chapter VII concludes with consideration of the analysis results as well as recommendations on where further research should be directed.

II. ELECTRIC SHIP DESCRIPTION

A. INTRODUCTION TO IPS AND ELECTRIC PROPULSION

The Navy continues to push for an all-electric ship that will employ an Integrated Power System (IPS). The IPS will provide a substantial increase in the electric power found in Navy ships today. The all-electric ship will employ electric prime movers instead of the mechanical gas turbine currently in use in most of the Navy's surface combatants. The IPS advantage allows it to use all its generators for propulsion and electrical load distribution. The increased power availability will enable the integration of electric weapons and systems such as the Free Electron Laser (FEL) and Rail Gun.

1. Historical Use of Electric Drives

The use of electric propulsion dates back to 1913, when it was first used on the Navy collier Jupiter (AC-3), which was later converted to the aircraft carrier USS Langley (CV-1) in 1922 [1]. The Langley's propulsion system consisted of steam-powered turbines driving generators, which supplied electrical power to Alternating Current (AC) propulsion motors [1]. The success of this turbo-electric AC drive system ensured its use with follow-on battleships and aircraft carriers, fifty vessels in all. DC electric drives were also used in many diesel submarines. These early electric drives were preferred over geared reduction because of the elimination of reversing turbines, reduction in the total number of turbines necessary, better fuel efficiency and reliability.

Electric drives were phased-out just prior to World War II in favor of geared turbine drives [1]. The geared

turbine drive held advantages in size and weight reduction over the electric drive [1]. Improvements in the metallurgy and manufacture of gears made possible this weight and size reduction [2]. Geared turbines also allowed for much higher speed [1]. The geared turbine drive has been used in the majority of surface warships since that time.

However, the capability of mechanical drives is approaching the limit of technology and affordability [2]. The advantages of the electric drive in the 1920's included performance, reduced manning and fuel efficiency [2]. These are the same advantages that the Navy would like to capitalize on today.

2. Future Use of Electric Drives

Advances in high-powered AC motors have enabled a possible return to electric drive propulsion. Various types of motors are under investigation for use in the IPS. Superconducting material used as the field windings of electric motors and generators will allow higher currents at low power levels.

The Navy announced the DD(x) program in 2001, which includes a family of advanced surface combatants, such as the advanced cruiser, CG(x), and the Littoral Combat Ship (LCS). IPS will be employed on these ships.

B. POWER GENERATION AND DISTRIBUTION

The Navy currently uses segregated power systems in most ships. The IPS will be different in that it will provide better flexibility for distribution of power to the electrical subsystems.

1. Segregated Power System

A segregated system consists of separate generators, to provide electrical power and propulsion. Figure II-1 shows a segregated power system.

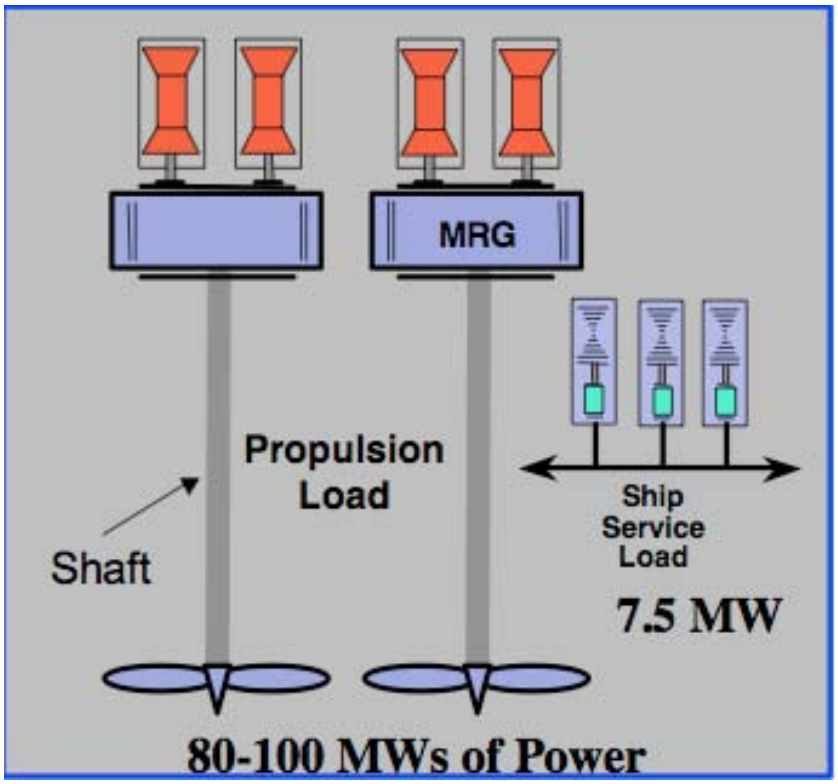

Figure II-1. Segregated Power System Currently in Use Onboard Many Navy Warships (From: NAVSEA).

The four prime movers or geared turbines (shown in red in the figure) are connected to a Main Reduction Gear (MRG). The MRG reduces the turbine speed down to an acceptable shaft speed, which allows the propeller to get the proper bight in the water. There are three generators (shown in cyan in the figure), which provide the ship's service load. The service load generators and the four prime movers are not cross-connected. Four Main Gas Turbine (MGT's) Generators are available for propulsion only, while three different generators are available to

provide the ship's electric power. This is a significant amount of weight and volume added to a ship. Additional weight, volume and cost, come from the separate auxiliary oil and cooling systems required to maintain these generators.

2. Integrated Power System

The IPS design will allow for integration of prime movers and service load generators. This will reduce the number of geared turbines required onboard. An Integrated Power system is shown in Figure II-2.

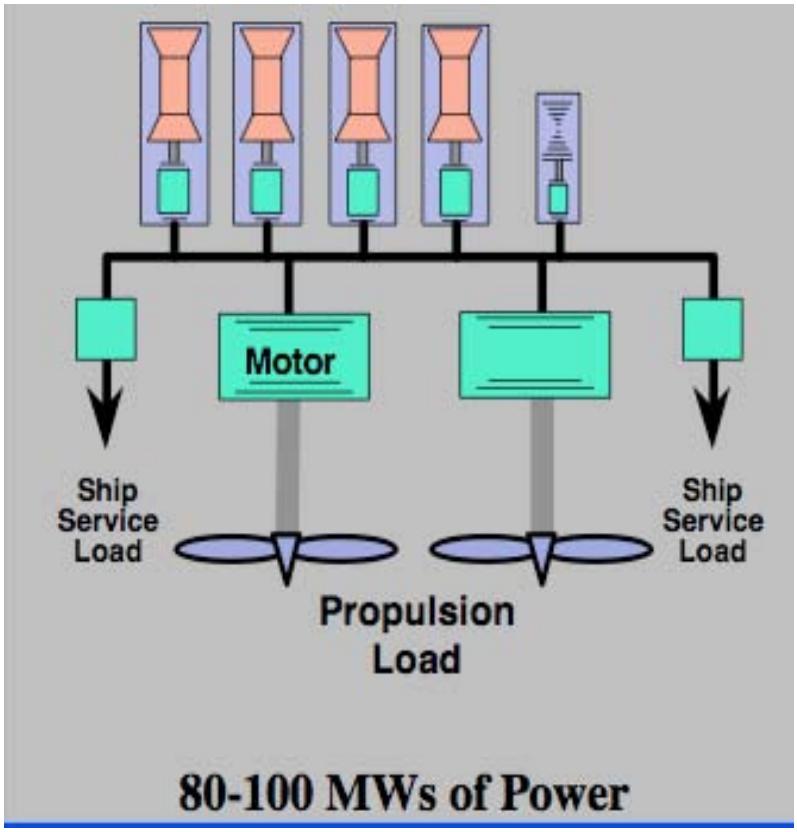

Figure II-2. Integrated Power System for Possible Use on Electric Ships (From: NAVSEA).

The number of generators required is only five, as seen in the figure, versus the seven in a segregated

system. The greater flexibility in distributing the electrical power is apparent, allowing the operators to cross connect individual turbines depending on the operational requirement placed on the ship. This allows for much better fuel efficiency and increased turbine generator life. Further effects of this power system arrangement including electric weapons will be discussed in Chapter VII using simulation software and operational scenarios.

C. PROPULSION OPTIONS FOR THE ELECTRIC SHIP

Two methods of electric propulsion being explored by the Navy are In-Hull and Pod propulsion. In-Hull propulsion is similar to the geared systems currently in use on modern ships. Pod propulsion is already being used on cruise liners and some commercial shipping.

1. In-Hull Propulsion

The prime mover in the In-Hull propulsion system is located inside the hull of the ship and attached to the shaft. Figure II-3 shows a picture of an in-hull propulsion setup. The prime mover transfers rotational torque to the propeller via the shaft. The prime mover is connected to the reduction gear, which in turn, is connected to the shaft. The shaft extends through bulkheads and to the exterior where the propeller is attached. The propeller converts rotational torque to thrust in the forward and reverse directions. Location of the prime mover is the deciding factor on the length of the shaft. With additional shaft length, additional support equipment is required. It already requires additional equipment for shaft bearings and bulkhead penetration equipment, such as shaft seals and a cooling system. Additionally, reversing turbines may be needed as well as

Controllable Pitch Propellers (CRP). CRP's change the pitch of the blades on the propeller to assist in speed changes without making turbine speed changes.

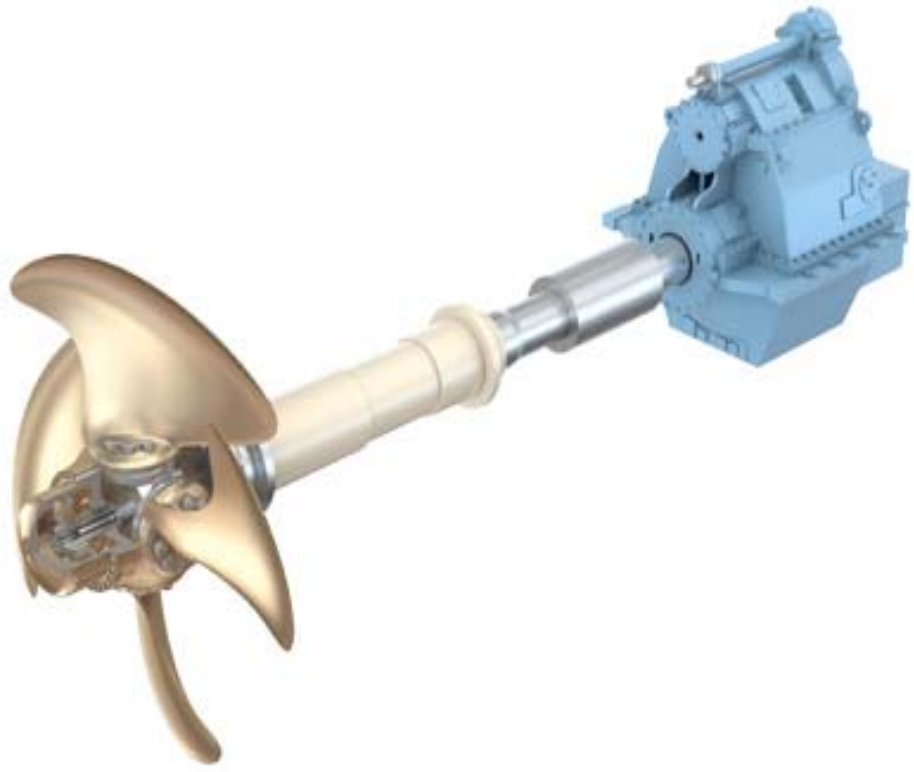

Figure II-3. Reduction Gear, Shaft and Propeller System to Demonstrate in-Hull Propulsion (From: Rolls-Royce).

2. Pod Propulsion

Pod propulsion makes use of Propulsors and are commonly used in the cruise liner industry and commercial shipping. The prime mover is located inside a pod located outside the ship's hull. This allows the propeller to be mounted directly to the prime mover, which eliminates the shaft and numerous support systems required for bulkhead penetrations. A prime mover can also be located inside the hull, which uses a gearing mechanism to connect the prime mover to the propulsor. A typical pod system is shown in Figure II-4. The Pods provide steering capability by

independently rotating through 360^{o}. This capability removes the need for a rudder and all associated support equipment.

Some of the benefits of using pod propulsion include increased efficiency and maneuverability, and increased design flexibility [3]. Fuel consumption reduction and propulsion efficiency can be increased by use of improved hull designed Pods [4].

Figure II-4. POD Propulsion Used on Commercial Shipping (From: Rolls-Royce).

Using pods can eliminate much of the auxiliary and support equipment associated with in-hull propulsion. Figure II-5 shows a pod system called Mermaid, manufactured by Rolls-Royce. In the pod system, the rudder, steering gear, propulsion motor, propulsion shaft, propulsion bearings and thrust bearings are all integrated into a single unit.

Figure II-5. Pod Propulsor Called Mermaid (From: Rolls-Royce).

III. PROBABLE ELECTRIC SHIP SYSTEMS

Electric ships bring the promise of increased power, capable of supporting such high-load weapons as the Railgun and FEL. These weapons may revolutionize the United States Navy in the Twenty-First Century. There are many other systems which bear on a ship's mission, such as sonar, radar and communication equipment, which may also be on the all-electric ship. FEL system description and theory is described in Chapter IV.

A. RAILGUN

Railgun technology is being pursued by both the U.S. Army and U.S. Navy. The railgun would make a suitable weapon for an all-electric ship having an energy storage system adequate to provide the gigawatt pulsed power required by the railgun.

1. Theory

A railgun operates using the principle of the Lorentz Force. The railgun uses the rails to carry a large current to create a magnetic field around each rail as shown in Figure III-1. These magnetic fields, in conjunction with the same current flowing through the moveable armature (positioned between the rails), produce a large force on the armature, which is used to propel the projectile down the rails. The following derivation gives an estimate of the force produced on a projectile as a function of an input current and rail geometry.

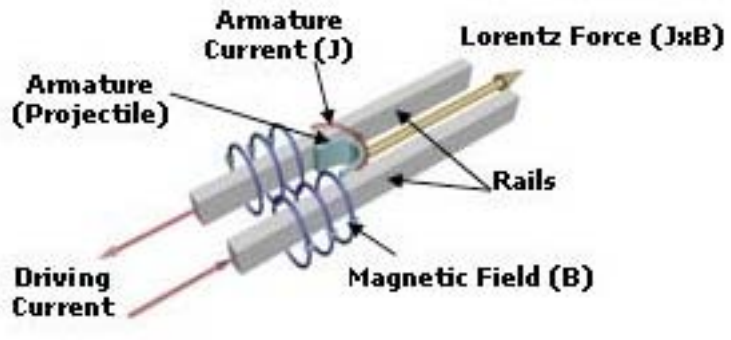

Figure III-1. Railgun Theory (From: ONR).

The force on an electron in MKS units is given by the Lorentz force equation

$$\vec{F} = q\vec{v}_d \times \vec{B}\,, \tag{3.1}$$

where *q* is the charge of the electron, v_d is the electron drift velocity and $\vec{B}$ is the magnetic field. The force on the projectile is found by summing the cross product of the currents and magnetic fields for each infinitesimal element along the length of the projectile. Each element of the projectile force is

$$d\vec{F} = dq(\vec{v}_d \times \vec{B})\,, \tag{3.2}$$

where *dq* is the charge at infinitesimal steps along the projectile and $\vec{B}$ is the magnetic field strength at a position along the projectile. The current flowing through two rails generates the magnetic fields, $\vec{B}_1$ and $\vec{B}_2$. For a semi-infinite wire, the magnetic field outside is given by the Biot-Savart Law:

$$B = \frac{\mu_o I}{4\pi x}\,, \tag{3.3}$$

where μ_o is the permeability of free space, I is the current through the wire and x, is the radial distance from the center of the wire.

When a projectile is placed between the rails on the armature, the current flowing through the armature at any one point experiences a different B-field strength from each rail. To find the total magnetic field strength along the projectile, the varying distances from the center of each rail must be included. Using equation (3.3) and these varying distances, the strength of the magnetic field from each rail contributes as

$$\vec{B}_1 = \frac{I\mu_o}{4\pi x} \tag{3.4}$$

$$\vec{B}_2 = \frac{I\mu_o}{4\pi(2R+w-x)}, \tag{3.5}$$

where x is the distance from the center of one rail to the infinitesimal width dx along the projectile length, w is the separation between rails and R is the radius of each rail, as shown in Figure III-2.

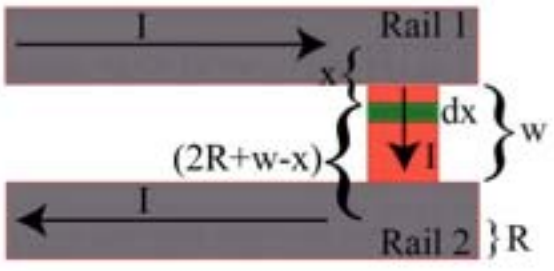

Figure III-2. Top view of rails showing distances used in calculations.

To understand the current elements traveling across the projectile, consider the charge element, dq, which may be expressed as follows

$$I = \frac{dq}{dt} \rightarrow dq = Idt \ . \qquad (3.6)$$

The infinitesimal change in time is given by

$$v_d = \frac{dx}{dt} \rightarrow dt = \frac{dx}{v_d} \ , \qquad (3.7)$$

where v_d is the drift velocity of the projectile, t is the time in seconds and dx is the distance along the projectile length. Substituting dt from equation (3.7) into equation (3.6), the elemental charge becomes

$$dq = \frac{Idx}{v_d} \ . \qquad (3.8)$$

We now substitute equations (3.4), (3.5) and (3.8) into equation (3.2) and integrate over the projectile, to give us the total force on the projectile as

$$F_p = \frac{\mu_o I^2}{4\pi} \int_R^{R+w} \left(\frac{1}{x} + \frac{1}{2R + w - x}\right) dx \ . \qquad (3.9)$$

After integrating, the total force is

$$F_p = \frac{I^2}{2}\left[\frac{\mu_o}{2\pi} \ln\left(\frac{(R+w)^2}{R^2}\right)\right] . \qquad (3.10)$$

The inductance gradient [L'], identified by the term in parenthesis in equation (3.10), remains constant once the railgun has been constructed. Thus:

$$L' \equiv \frac{\mu_o}{2\pi} \ln\left(\frac{(R+w)^2}{R^2}\right) . \qquad (3.11)$$

Substituting equation (3.11) into (3.10), the Lorentz force on the railgun projectile can be written as

$$F = \frac{1}{2} L' I^2 . \qquad (3.12)$$

The force on the projectile can now be calculated by simply inserting the current into the equation. Knowing the projectile mass and current, the calculated force allows us to find the acceleration and hence, the muzzle velocity.

2. Power

The nominal Naval railgun has been chosen with the approximate maximum range of 360 km and with energy on target of 17 MJ. The railgun is expected to draw approximately 20 GW of pulsed power from the onboard energy storage system. Energy storage systems will be discussed in Chapter V, but the expected energy draw of a flywheel energy storage system from the IPS is approximately 40 MW while charging. The peak power draw of the railgun will be much higher and is estimated to be 20 GW. This requires about 160 MJ of total energy delivered to the railgun for a pulse-width of 8 ms. This pulsed power must be provided by an energy storage unit, which is discussed in more detail in Chapter V.

B. ADVANCED MULTIFUNCTION RADIO FREQUENCY CONCEPT (AMFRC)

The Advanced Multifunction Radio Frequency Concept (AMFRC) is the integration of many shipboard Radio Frequency (RF) functions including radar, communications and Electronic Warfare (EW) utilizing a common set of broadband array antennas as shown in Figure III-2 [5]. This system was not part of the Electric Ship Simulation presented in Chapter VI, but is introduced here to consider

its inclusion in the next study. Radar loads were used in the simulation results presented in Chapter VI, but they were generic loads not representative of any known radar system. Once more data is collected on AMFRC, models could be built using Simulink® and used in further simulation models.

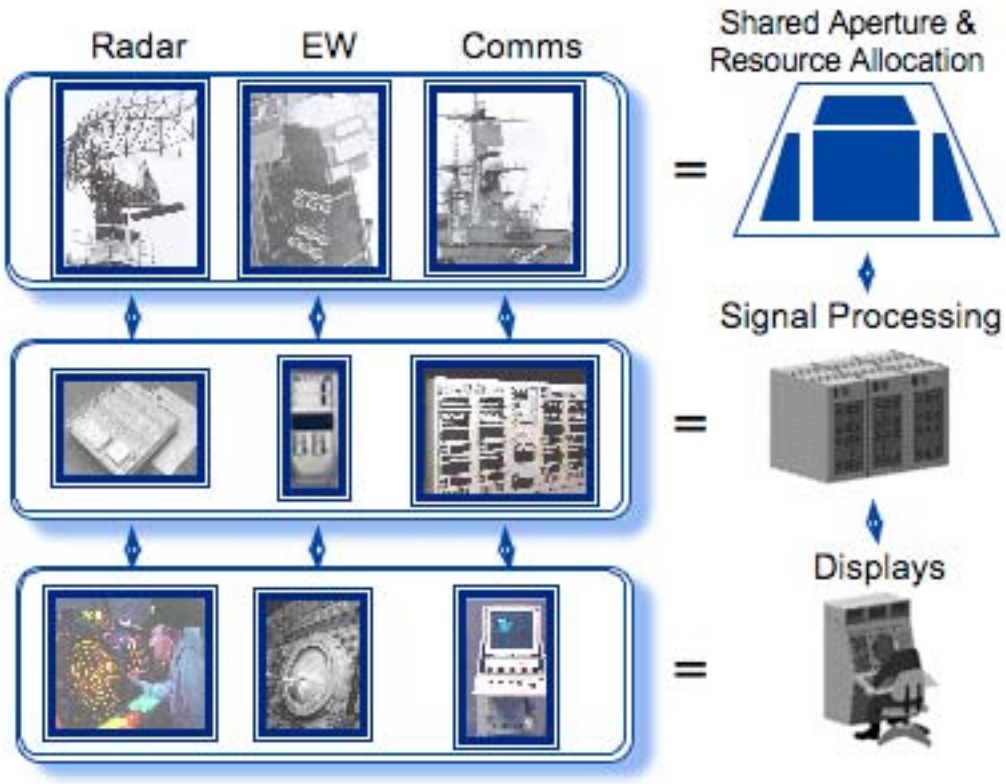

Figure III-3. AMFRC Concept of Reducing Sensors (From ONR).

Advantages of AMFRC include: reduced number of topside antennas, thereby, reducing the ship Radar Cross Section (RCS) and infrared (IR) signature; potential for expansion without adding additional apertures; reduction in life cycle costs.

IV. FREE ELECTRON LASER COMPONENTS AND THEORY

The Free Electron Laser (FEL) will have a primary mission on board naval vessels as a close-in missile defense system. It can also be used in an area defense scenario as well as missions against small boats and small aircraft. The FEL mission can be extended to a shore support role directly or by use of relay mirrors.

A. AUXILIARY SYSTEMS

There are many factors to consider when designing a new weapon system for use onboard a ship. The overall consideration for any system is to ensure that it works properly and safely. Other factors to consider include the size, weight, cost, power requirements and cooling.

1. Power

Like many systems on a naval combatant, an FEL requires a large amount of input power to operate effectively. Depending on the power of the weapons class laser, this power consumption can vary from an estimated 10 MW to 40 MW. For example, a 3 MW class laser requires approximately 20 MW of power during an engagement. The 3 MW FEL may be required to conduct 3 to 5 engagements, each lasting 5-7 seconds, in a matter of minutes. It is easy to see that a very robust prime power system is required to support a shipboard FEL. Chapter II focused on the proposed Electric Ship power distribution system, which can support a shipboard FEL. Specific simulation results will be presented later.

2. Secondary/Auxiliary Power

The FEL may require an energy storage system to support it, as do other electric devices onboard such as a

Rail Gun or Electromagnetic Aircraft Launch System (EMALS), each of which requires a large amount of pulsed power. This pulsed power must come from a primary power system and may be shared among various loads. It can come from several possible energy storage devices, such as capacitors, batteries, Superconducting Magnetic Energy Storage (SMES) or rotating machinery (alternators). The various possibilities will be explored in Chapter V. The integration of normal ship's power with pulsed power is also a challenge and will be examined further in Chapter VI.

3. Electron Beam Injector

The electron beam injector uses a cathode, and is the original source of electrons within the FEL. The cathode is positioned within a Radio Frequency (RF) cavity, and a high voltage is applied that accelerates electrons from the cathode. The beam of electrons from the cathode leave the RF cavity and enter the accelerator.

Figure IV-1 shows an artists' rendering of the Injector Module that Thomas Jefferson National Laboratory (JLAB) is currently developing in collaboration with Advanced Energy Systems (AES). The module is a 100 mA injector consisting of a superconducting RF gun operating at 750 MHz, providing a bunch charge of 135 pC. Each accelerating module in the injector is made up of three single-cell cavities with an energy gain of 2.5 MeV per cavity for an overall gain of 7.5 MeV [6].

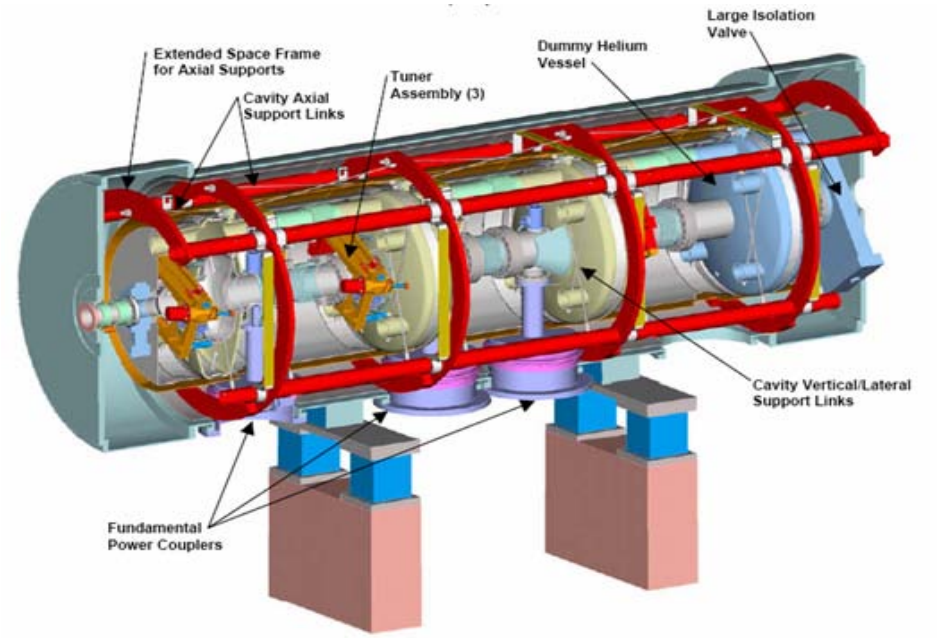

Figure IV-1. JLAB Injector Module (From: Jefferson Laboratory).

4. Accelerator

The electrons from the injector have energy around 7.5-10 MeV. These electrons are then accelerated to an energy level of 100 MeV. To attain this energy level, the electron beam is passed through a Superconducting Radio Frequency Linear Accelerator (SRF LINAC). The electrons accelerate through several stages of superconducting RF accelerator modules until the required energy gain is accomplished.

These accelerator modules contain about eight accelerator cavities. Each cavity contains several shells which are shaped to produce the RF field for acceleration of the electrons. The acceleration gradient is about 10 MeV per meter for the JLAB module [7]. So, for example, if each cavity is one meter in length, it will take about nine of the cavities to accelerate the electron beam from 10 MeV to 100 MeV.

The electromagnetic field, which accelerates the electron beam, is generated by a klystron. The RF field, which does the acceleration, is synchronized with the photo-injector's mode locked laser and oscillates at the frequency of 750 MHz. An alternating electric field interacts with each electron bunch that travels down the cavity. The field is in synchronism with the electron bunches so that it continuously accelerates the electrons.

Figure IV-2 shows a recirculating-beam FEL system in which the injector and accelerator are shown, the undulator or wiggler and mirrors will be discussed in section B.

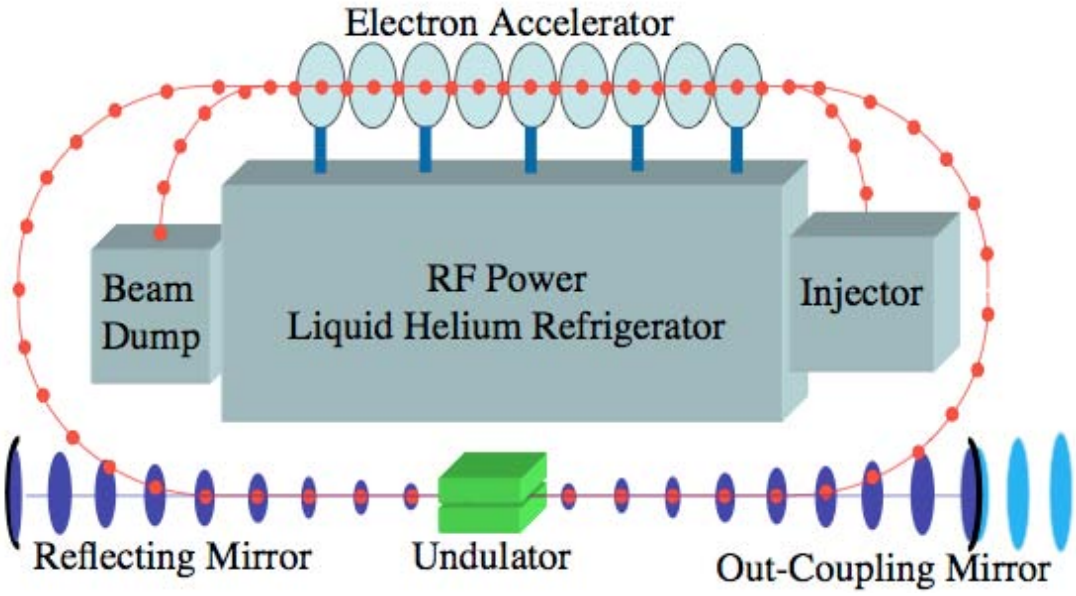

Figure IV-2. Recirculating-Beam FEL System (From: Colson, NPS).

5. Refrigeration

A cryomodule encases the superconducting RF accelerator and is kept cool to approximately 2 K by use of a liquid helium refrigerator. Size of the refrigeration equipment depends on the cooling rate required. The system

will be cooled from room temperature (300 K) down to 2 K in port and could require a large time (days). After cooling, the refrigerators onboard ship maintains the low temperature. Additional cooling is only required after the FEL operates. System maintenance cooling is expected to require about 1 MW. It is possible to have a refrigerator that operates the FEL continuously.

Figure IV-3. Cryomodule at JLAB (From: Jefferson Laboratory).

Figure IV-3 shows the cryomodule currently in use at JLAB. Consideration of operational requirements of the FEL will ultimately dictate the size of the refrigeration equipment.

B. OPTICAL LIGHT/ENERGY GENERATION

Once the electrons are accelerated to full energy of about 100 MeV, they can be used to generate light. After the electrons leave the accelerator, they are introduced to

the undulator and optical cavity. The static magnetic field of the undulator forces the electrons to oscillate in a transverse direction, which causes the electrons to radiate light. This optical energy is then passed on to the beam director on the deck of the ship.

1. Undulator

Once the electron beam reaches the undulator, the beam energy is sufficient to produce an optical beam. The electron beam undergoes oscillation inside the undulator due to the periodic magnetic field set up by permanent magnets that alternate in polarity. The periodic motion causes the electrons to radiate at a predictable wavelength, related in a simple way to the undulator period. The wavelength can be changed by manipulation of the magnetic field strength or the electron beam's energy. It is easy to see a major advantage of the FEL is that the output wavelength is tunable, which provides some design flexibility to the overall weapon system.

2. Optical Cavity

Two mirrors are positioned at each end of the optical cavity, which is oriented along the longitudinal axis of the undulator. The mirror spacing is adjusted to ensure the reflected light pulse is synchronized with the electron pulses entering the undulator from the accelerator. The light pulse is repeatedly reflected between the mirrors, amplifying the light to produce the optical beam.

Figure IV-4 shows the optical cavity and the undulator it contains. The mirror at the right is partially transmissive in order to allow the light to be extracted from the optical cavity. Only a fraction of the light actually escapes and this light is the laser beam's output.

The remaining energy of the electron beam is recirculated back into the system, which increases efficiency and reduces beam dump size.

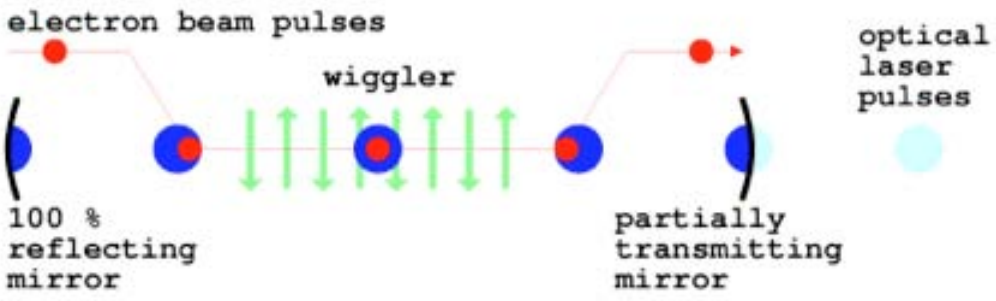

Figure IV-4. Optical Cavity (From: Colson, NPS).

The FEL can operate, alternatively, as an amplifier rather than an oscillator. The single-pass amplifier starts with a seed laser, eliminating the resonator mirrors.

C. LIGHT TRANSPORT

The laser light generated is sent into the atmosphere to a potential target. The location of the FEL onboard a naval surface ship will dictate the required routing of the light. Most likely, the FEL will be located low in the ship, which means that the light will traverse through several bulkheads to reach the beam director. The beam director, as controlled by a fire control system, will direct the laser beam toward the target.

1. Beam Guide

The laser beam will leave the optical cavity through the partially transmissive mirror and into the beam guide, which routes the laser beam through the ship to the director. The beam guide will be much like a microwave waveguide currently used on board naval vessels for radar.

However, the laser beam will be focused to travel along the center of the beam pipe without touching the side. It may be evacuated to prevent loss of laser beam energy. This ability to provide a near zero pressure in the beam pipe is routine technology onboard ships and will not be a major obstacle for the FEL to overcome.

The reflective mirrors located inside the beam guide must reflect the laser beam at high energy without a loss of beam quality, but the power of this laser beam is sufficient to melt almost anything. Whatever method to prevent these mirrors from melting must not require monitoring by shipboard technicians. Cooling the mirrors and spreading the beam over a larger mirror area could prevent melting.

2. Beam Director

The beam director takes the laser beam from the beam guide and directs it through the atmosphere to the target. It will be used in conjunction with a fire control system capable of steering the beam director in azimuth (bearing or direction) and elevation (altitude). Figure IV-5 shows the beam director for the Tactical High Energy Laser (THEL). The beam director will focus the laser beam onto the target and keep it on target for the duration of the engagement, possibly several seconds. The beam director may also have built-in detectors for calculation of atmospheric parameters, which can be used to adjust its internal adaptive optics, and reduce the effects of atmospheric turbulence on the quality of the laser beam at the target.

Figure IV-5. THEL Beam Director (From: Northrup Grumman).

D. FREE ELECTRON LASER THEORY

We now show, using classical electromagnetic theory, how the accelerating electrons produce laser light [7].

1. Undulator Fields and the Resonance Condition

The forces that affect the electrons as they travel through the undulator arise from: (a) the static magnetic field from the undulator magnets, and (b) the electric and magnetic fields of the optical beam. An electron enters the helical undulator field traveling along the z-axis. It sees the undulator field,

$$\vec{B} = B(\cos(k_o z), \sin(k_o z), 0)\,, \tag{4.1}$$

where $\lambda_o = 2\pi/k_0$ is the undulator period and B is the magnetic field strength. The corresponding optical beam fields are

$$\vec{E} = E(\cos\psi, -\sin\psi, 0)\,, \tag{4.2}$$

and

$$\vec{B} = E(\sin\psi, \cos\psi, 0)\,, \tag{4.3}$$

where $\psi = kz - \omega t + \phi$, E is the optical field amplitude in cgs units, ϕ is the phase, $k = 2\pi/\lambda$ is the wavenumber, λ is the wavelength, and ω is the optical frequency. Therefore, the overall motion is determined by the relativistic Lorentz force equations [8]

$$\frac{d(\gamma\vec{\beta})}{dt} = -\frac{e}{mc}(\vec{E} + \beta \times \vec{B})\,, \tag{4.4}$$

$$\frac{d\gamma}{dt} = -\frac{e}{mc}\vec{\beta} \bullet \vec{E}\,, \tag{4.5}$$

$$\gamma^{-2} = 1 - \vec{\beta}^2\,, \tag{4.6}$$

where $\vec{v} = \vec{\beta}c$ is the electron velocity, m is the electron mass, $e = |e|$ is the electron charge magnitude and γ is the relativistic Lorentz factor.

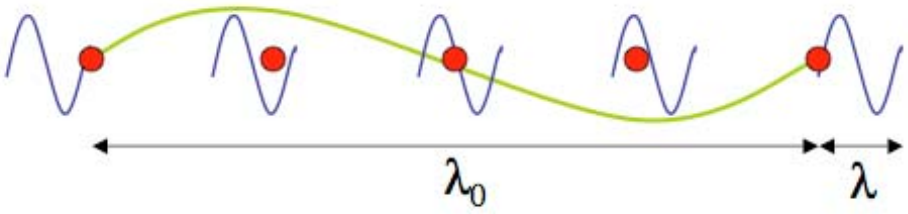

Figure IV-6. Electron in Resonance Condition (From: Colson, NPS).

As the electrons travel the length of the undulator, they interact with the fields (4.1), (4.2) and (4.3). The electron position and velocity have a certain relationship

with the optical and undulator fields, which is required for laser beam amplification. This "resonance condition", requires that as the electron travels a distance λ_o, the light wave travels a distance $(\lambda_o + \lambda)$, where λ is the output wavelength given by

$$\lambda = \lambda_o \left(\frac{1 + K^2}{2\gamma^2} \right), \tag{4.7}$$

where $K = (eB\lambda_o / 2\pi mc^2)$ and is known as the undulator parameter [7]. The sequence of electron positions (red) along one undulator period λ_o (green) is shown in Figure IV-1. A wavelength of laser light (blue) passes over the electron at resonance. The FEL wavelength can be adjusted by changing the undulator period, the undulator strength or the electrons beam energy.

2. The Pendulum Equation and Electron Motion

When an electron enters the undulator of an operating FEL, its microscopic motion is determined by the undulator and laser fields together. Equations (4.4) through (4.6) include a total of five equations with four unknowns. Substitution of the undulator and laser fields into (4.4) gives the transverse components of the electron motion:

$$\frac{d(\gamma\beta_x)}{dt} = -\frac{e}{mc}(E(1-\beta_z)\cos(\psi) - B\beta_z \sin(k_o z)), \text{ and} \tag{4.7}$$

$$\frac{d(\gamma\beta_y)}{dt} = -\frac{e}{mc}(-E(1-\beta_z)\sin(\psi) + B\beta_z \cos(k_o z)). \tag{4.8}$$

For relativistic electrons, $\beta_z \approx 1$, so that $E(1-\beta_z)$ is small compared to $\beta_z B$. After combining (4.7) and (4.8) and integrating, the transverse velocity of a perfectly injected electron is

$$\vec{\beta}_{\perp} = -\frac{K}{\gamma}(\cos(k_o z), \sin(k_o z), 0) \,. \tag{4.9}$$

The rate of charge of the electron energy is found from (4.5) combined with (4.9) to be

$$\dot{\gamma} = \frac{d\gamma}{dt} = \frac{eKE}{\gamma mc}\cos(k_o z + \psi), \tag{4.10}$$

where the electron phase is defined as

$$\zeta = (k + k_o)z - \omega t \,. \tag{4.11}$$

A change in the electron energy (γ) results in a change in the electron phase (ζ) by

$$\frac{d\gamma}{dt} = \left(\frac{\gamma}{2k_o c}\right)\frac{d^2\zeta}{dt^2} \,. \tag{4.12}$$

The equation of motion for an electron then becomes

$$\frac{d^2\zeta}{dt^2} = 2k_o \frac{eKE}{\gamma^2 m}\cos(\zeta + \phi) \,. \tag{4.13}$$

The electron phase velocity is defined

$$\nu = \mathring{\zeta} = L[(k + k_o)\beta_z - k], \tag{4.14}$$

where $L = N\lambda_o$ is the length of the undulator, and $\mathring{()} = {}^{d()}\!/_{d\tau}$ indicates a derivative with respect to dimensionless time (τ). The dimensionless time along the undulator is $\tau = ct/L$, so that $\tau = 0 \to 1$ along the undulator length. The motion of the electrons is given by the pendulum equation

$$\ddot{\zeta} = \dot{\nu} = |a|\cos(\zeta + \varphi), \tag{4.15}$$

where $|a| = 4\pi NeKLE/\gamma^2 mc^2$ is the dimensionless laser field amplitude [7].

3. The Wave Equation

To fully understand FEL theory, electrons and the optical beam interaction with the optical wave must be understood. This involves the slowly-varying wave equation where the current source is due to the bunching electron beam in the FEL optical wavefront. The vector potential for the optical field is [7]

$$\vec{A} = \frac{E}{k}[\cos(\psi), -\sin(\psi), 0], \tag{4.16}$$

where the amplitude and phase of the electron radiation vary slowly in time and space. The full wave equation is then

$$\left(\vec{\nabla}^2 - \frac{1}{c^2}\frac{\partial^2}{\partial t^2}\right)\vec{A} = -\frac{4\pi}{c}\vec{J}_\perp, \tag{4.17}$$

where $\vec{J}_\perp =$ transverse current density due to oscillations of the electrons passing through the undulator [8]. Substituting (4.16) into (4.17), the wave equation with a slowly varying amplitude and phase can be written as

$$\frac{\partial}{\partial t}(Ee^{i\phi}) = -\frac{2\pi Kec\rho_e}{\gamma}\left\langle e^{-i\zeta}\right\rangle, \tag{4.18}$$

where $\rho_e =$ electron beam particle density and $\langle .. \rangle$ is an average of sampled electron phases ζ. Introducing the dimensionless field amplitude definition $|a|$ and dimensionless time τ, defined in the last section, the FEL wave equation can be written in its simplest form is

$$\frac{\partial a}{\partial \tau} = \overset{\circ}{a} = -j\left\langle e^{-i\zeta} \right\rangle, \tag{4.19}$$

where the dimensionless current is

$$j = \frac{8\pi^2 K^2 L^2 N e^2 \rho_e}{\gamma^3 mc^2}, \tag{4.20}$$

where $L = N\lambda_o$ and N=number of undulator periods [7].

The dimensionless current j is an important FEL parameter and measures the coupling between the laser light and electron beam, while the average $\left\langle e^{i\zeta} \right\rangle$ measures the amount of bunching in the beam. When the electrons are randomly spread in ζ, the average is small and the coupling between the light and electrons is small. When the dimensionless current is small, $j \le \pi$, the FEL coupling is small. When dimensionless current is large, $j \gg \pi$, the coupling is large and there is high gain.

4. FEL Gain and Phase Space Plots

a. Gain

From (4.10) and (4.20), it can be seen that electrons will both lose and gain energy during the interaction along the undulator. In order to obtain net gain, the electrons must contribute more energy to the optical beam than they absorb. Optical gain is the fractional energy increase of the optical beam during a single pass through the undulator and is defined by

$$G(\tau) = \frac{\left|a(\tau)\right|^2 - a_0^2}{a_0^2}, \tag{4.21}$$

where a_0 is the initial dimensionless optical field strength at the beginning of the undulator and $a(\tau)$=dimensionless optical field strength along the undulator. At $\tau = 1$, we have the final Gain G.

b. FEL Phase Space Evolution in a Strong Field

In the case of the FEL, phase space represents the microscopic motion and bunching of the electrons traveling through the undulator. A phase space plot from an FEL, as shown in Figure IV-7, plots electron phase velocity $\nu = \overset{o}{\zeta}$ versus the microscopic electron phase ζ from the pendulum equation (4.15). Evolution of the optical phase $\phi(\tau)$ and the optical gain $G(\tau)$ are plotted at right from the wave equation (4.19) evolving from $\tau = 0$ to $\tau = 1$. For amplification of the optical wave, the electrons must bunch around $\zeta + \phi = \pi$. In the case shown, the electrons have started at resonance, so that maximum bunching occurs at phase $\zeta + \phi \approx \pi/2$, resulting in small gain G and a large optical phase shift ϕ. In order to achieve net gain, $G \approx 0.135j$, the electrons must start slightly off-resonance at $\nu_0 \approx 2.6$, so that bunching occurs at phase $\zeta + \phi \approx \pi$. This case is not shown, but would be the optimum for FEL operation [7].

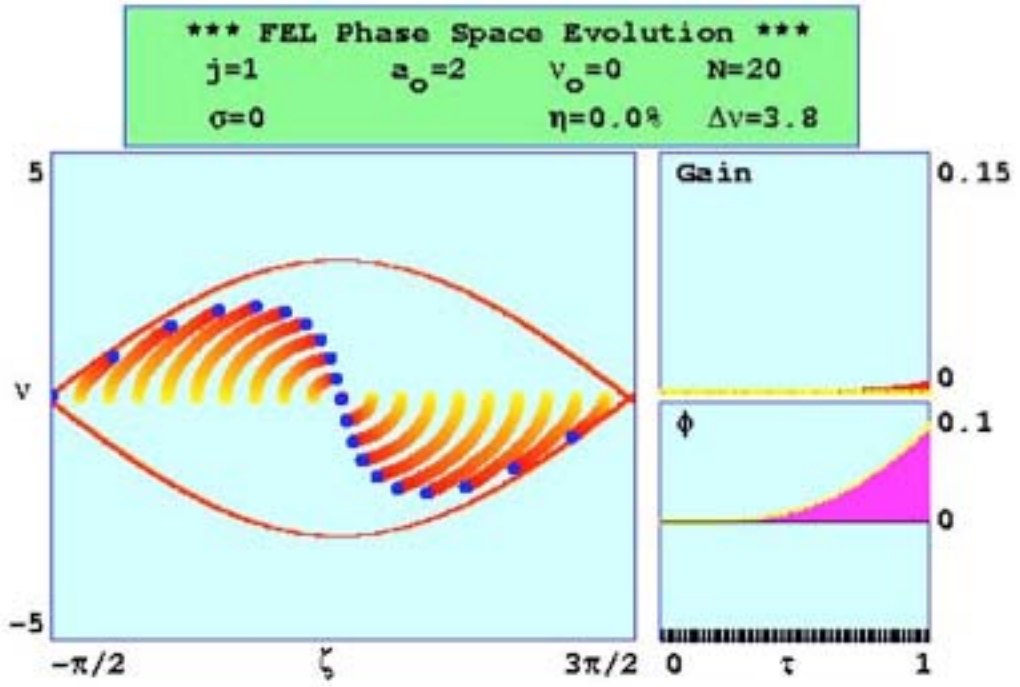

Figure IV-7. Phase Space Evolution (From: Colson, NPS).

V. PULSE POWER CONSIDERATIONS

The new weapon systems that could potentially be installed onboard an electric ship have been discussed as well as their respective power requirements. The fundamental question remaining is to determine the optimum pulse power system, which will (a) meet the requirements for each of these weapons and (b) enable the weapon systems to share the power. Benefits of sharing include a reduction in weight and ease of integrating future electric weapons; however, operations may be affected. Chapter VI will employ a simulation to explore the operations of these weapon systems.

There are currently several pulse power storage possibilities being researched: inertial rotating machines (flywheels), capacitors, Superconducting Magnetic Energy Storage (SMES) and batteries. The pulse power device chosen by the Navy for EMALS is the flywheel.

A. FLYWHEELS (INERTIAL MACHINES OR PULSED ALTERNATORS)

Flywheels have been used commercially for many years, although, compared to capacitors, the technology lags. However, flywheels are capable of high energy densities. A flywheel consists of a motor, a generator, and a rotating mass that stores kinetic energy to drive the generator. Figure V-1 shows a drawing of a flywheel assembly.

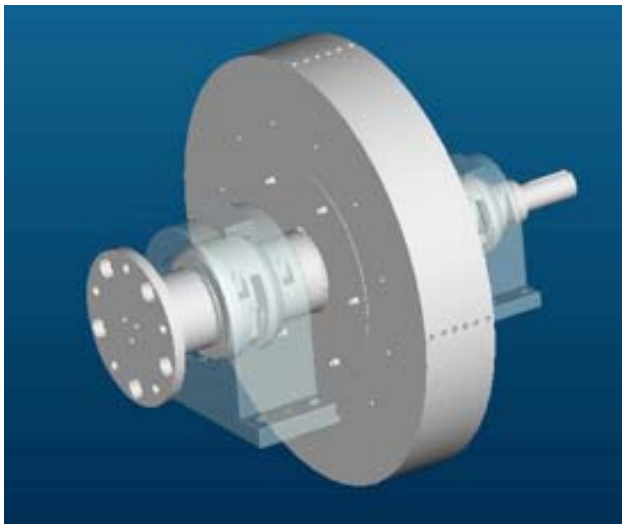

Figure V-1. Flywheel Assembly Drawing (From: CEM)

The mass required in the flywheel depends on how it is distributed. If it is distributed uniformly in a disk, then the Moment of Inertia (I) is

$$I = \frac{mr^2}{2}, \tag{5.1}$$

where m is the rotor mass, and r is the radius of the rotor. The resulting stored kinetic energy is given by

$$E = \frac{I\omega^2}{2}, \tag{5.2}$$

where ω is the angular velocity of the rotating mass in radians/s. The field winding wrapped around the generator rotor is energized, and current is passed into the field winding via brushes located on the shaft of the rotor. This current creates a magnetic field that crosses the armature windings of the stator. A current is then generated within the stator windings that can be used to supply pulsed power to weapon systems such as the Rail Gun and FEL.

Flywheels will provide pulsed power to the EMALS system installed aboard aircraft carriers. The EMALS system will replace the steam catapults now in use. The pulse power for EMALS is stored kinetically in the rotors of the alternators. The energy is then released in bursts of 2-4 seconds per launch. Between bursts, the rotor assembly operates as a motor alternator energized by the ship's power to spin up in the seconds between successive launches. Advantages of this type of pulse power for EMALS include reliability, high energy density and an ability to store energy for large periods of time without the lifespan reduction seen in batteries and some capacitors. These advantages could be beneficial over other pulse power options for the FEL and Rail Gun as well.

B. CAPACITORS

A capacitor ia an electrical device, which consists of two conducting plates of area A, one with a charge $+Q$ and the other $-Q$, separated at a distance d by an insulating material called a dielectric, as seen in Figure V-2.

The capacitor stores electric energy between the plates in the dielectric in the form of electrical fields. This energy can be recovered later when needed and then the capacitor can be recharged and used again as a pulsed power provider.

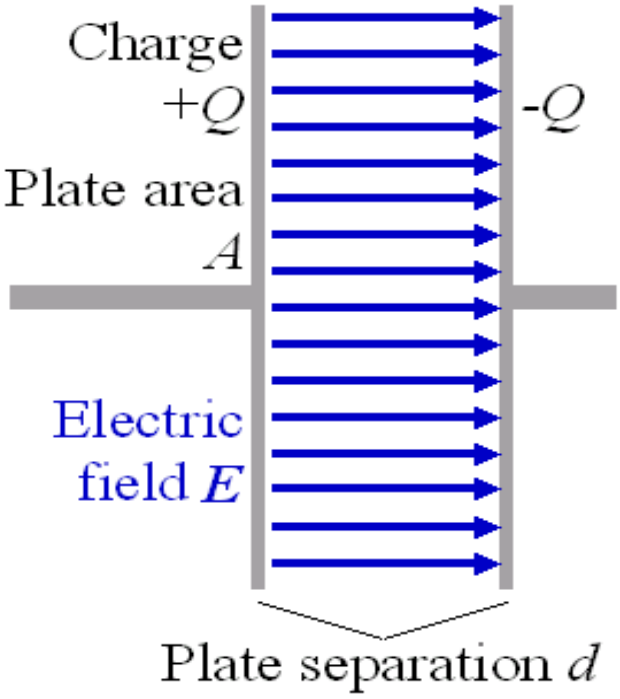

Figure V-2. Capacitor Schematic.

The capacitance *C* of a parallel plate capacitor is

$$C \approx \frac{\varepsilon A}{d}, \tag{5.3}$$

for $A \gg d^2$. The permittivity ε is dependent upon the material being used as the dielectric. The energy stored in a capacitor is

$$E = \frac{1}{2} C V^2, \tag{5.4}$$

where the potential difference *V* between the two plates is $V = Q/C$.

Capacitors have a high energy density, and their characteristics are well known, which make them excellent candidates for use as pulsed power sources. An additional advantage of the capacitor is that it has no moving parts,

which simplifies maintenance. Capacitor bank modularity allows for easy replacement. The major drawback is its overall lifetime, which can be reduced due to current leakage. Leakage occurs due to high-voltage spikes or excessive voltage, which may actually puncture the dielectric material. The longer a charge is held across a capacitor, the greater the leakage currents, so rapid charge and discharge maximize the lifetime.

Ultra-capacitors are new variations of capacitors, and double layered to provide much higher energy densities at lower voltages. Ultra-capacitors also have higher energy densities but may have heating issues. They are more reliable, can be cycled many more times than capacitors and hold their charge for months.

C. SUPERCONDUCTING MAGNETIC ENERGY STORAGE (SMES)

Superconducting Magnetic Energy Storage is the least mature technology under consideration for use onboard electric ships. SMES uses a large inductor made of a superconducting material that has been cryogenically cooled. The energy comes from the magnetic field created by the flow of direct current in the coil wrapped around the inductor. A SMES block diagram is shown in Figure V-3. The direct current flows into the superconducting coil, increasing the magnetic field strength. The energy stored by this circuit is

$$E = \frac{1}{2} LI^2, \tag{5.5}$$

where L is the inductance in Henrys and I is the current in amperes. The big advantage of the SMES over capacitors is that the energy can be maintained for an indefinite period of time. The SMES can recharge within minutes and repeat

the charge/discharge cycle thousands of times without any loss or degradation to components. Recharge time can be adjusted based on the needs of the load.

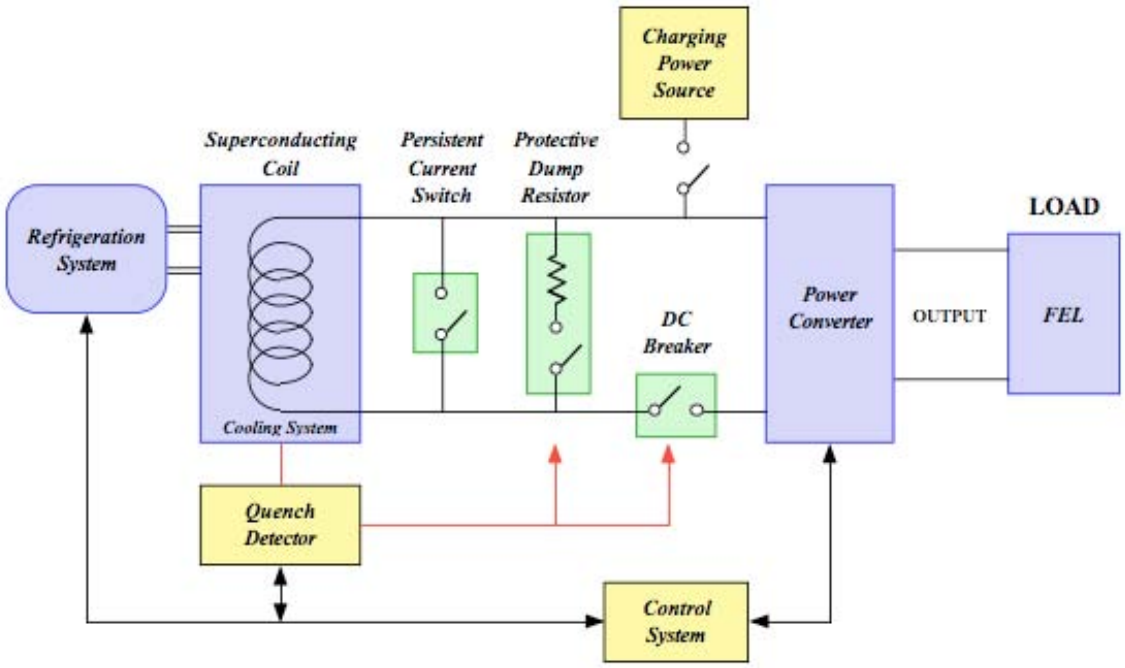

Figure V-3. Block Diagram of SMES (From: mPower).

However, the energy density is very low compared to capacitors and flywheels. The SMES would become very large for the power needed, especially if supplying both the Rail gun and the FEL. It may also affect the magnetic signature of the ship.

D. BATTERIES

Batteries work in much the same way as capacitors. They have two plates, which have a material between them, such that a chemical reaction produces opposite charges on the two plates. The plates then form positive and negative terminals, with a potential difference between them. Electrons collect on the negative terminal of the battery

and when a load is connected to both terminals, these electrons flow from the negative to the positive terminal as current.

The energy density of a battery is relatively low compared to the other energy storage options. Additionally, the cell life of a battery is extremely short and batteries have thermal management issues to address as well.

E. SUMMARY

Choosing the correct energy storage device focuses on tradeoffs between cost, weight, energy and power densities as well as charge/discharge times.

Figure V-4 is called a Ragone plot and it shows the energy density versus the power density of the energy storage devices.

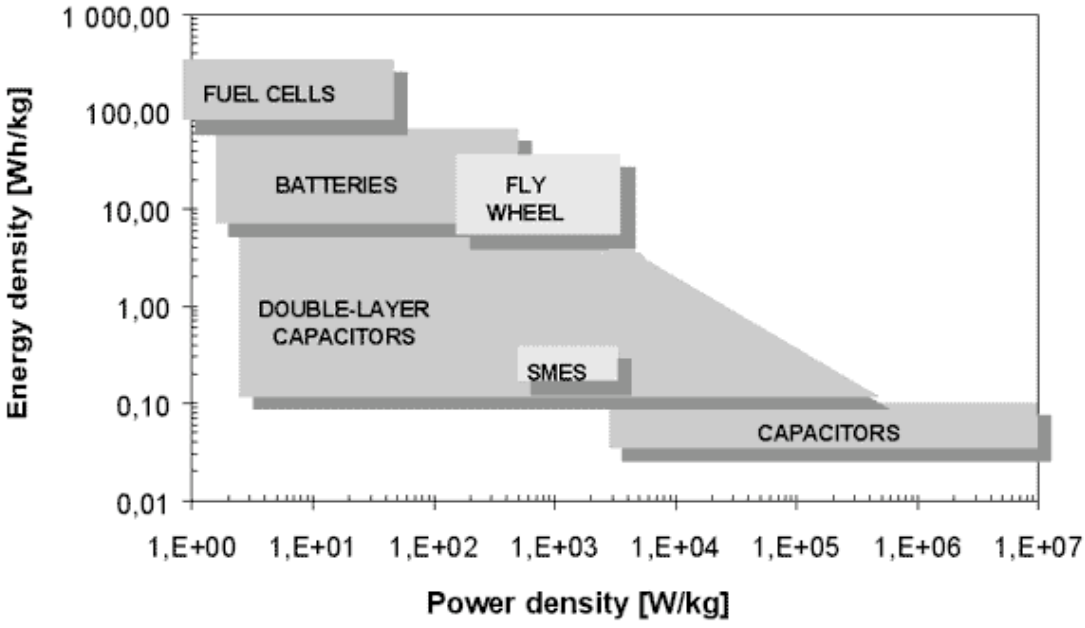

Figure V-4. Ragone Plot Showing Energy Storage Devices (From: mPower).

The figure indicates the best choice for high power applications, such as the FEL and Railgun, is the flywheel. Initial cost estimates for these systems also show the flywheel to be less expensive compared to other pulse power possibilities costing approximately 100 million dollars. The flywheel is a modular device, which can be scaled by adding more flywheels to the desired power application. It is not necessary to simply make a bigger flywheel. The low maintenance cost over the life of a flywheel system may offset its initial high cost.

VI. ELECTRIC SHIP SIMULATION

A. POWER SYSTEM SIMULATION

To simulate the behavior of proposed electric weapon systems such as the FEL or Railgun, it is necessary to assume a hypothetical ship power system. Figure VI-1 is the power system used in these simulations.

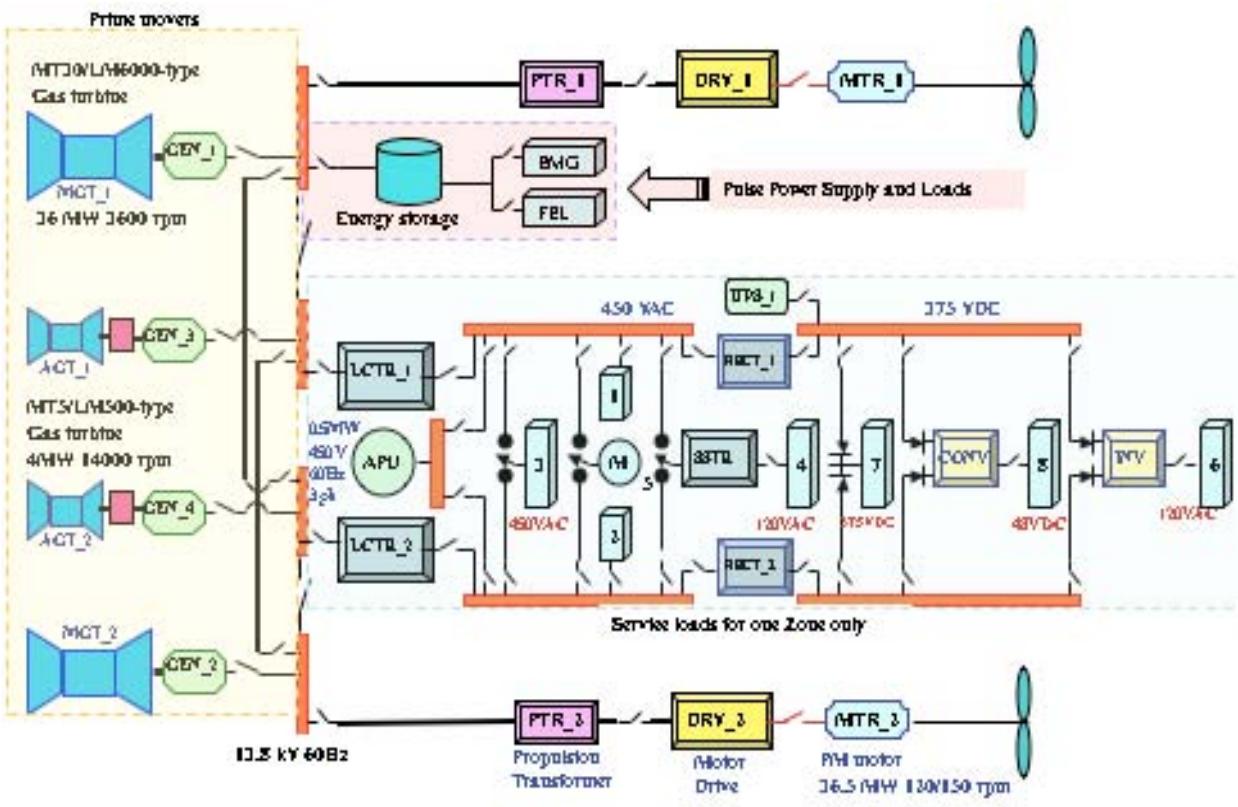

Figure VI-1. Notional Power System (From: CEM).

This depiction does not reflect a known Electric Ship power system, but it is a good starting reference for a power system with enough complexities to study power effects of FEL's and Railguns.

The system being simulated is an Integrated Power System (IPS) containing a total of four Gas Turbines. Two Main Gas Turbines (MGT's) are providing 36MW at 13.8 kV

line-to-line voltage while the two Auxiliary Gas Turbines (AGT's) provide 4MW of power at the same line-to-line voltage. The model also contains port and starboard propulsion trains. The propulsion trains can use power from either of the MGT's or AGT' and any combination of generators. At a maximum speed of 30 knots, the propulsion Trains consume approximately 74 MW, leaving only 6 MW for ship service loads.

Figure VI-2 shows a simulation of a specific scenario. A ship is traveling at 10 knots initially, then increasing speed to 30 knots. At 86 seconds, a MGT malfunctions and the ship must rely on the three remaining turbines for propulsion and hotel loads, such as other lights and other electrical equipment. With the loss of one MGT, the ship is limited to 120 shaft rpm, which corresponds to approximately 25 knots.

The hotel loads in the simulation can be changed based on the ship's operational scenario. Additional loads include two energy storage devices (ES1, ES2). These two devices provide pulsed power to the Railgun and for this simulation, also provide the FEL required pulsed power.

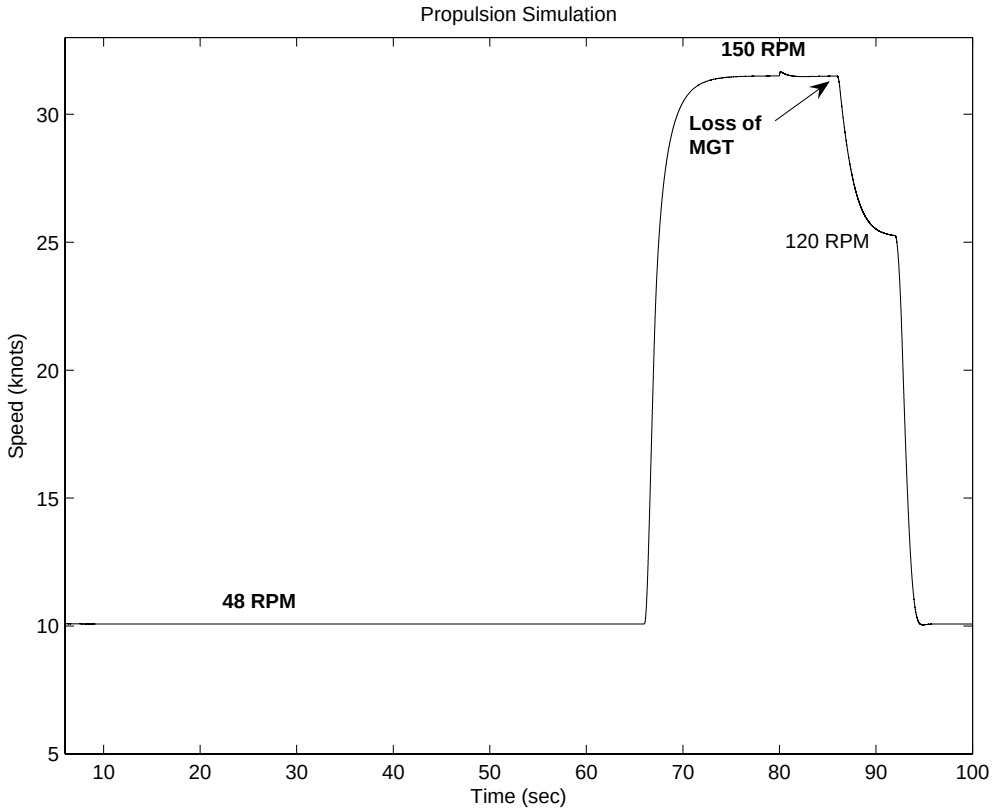

Figure VI-2. Propulsion Simulation Using SIMULINK®.'

B. RAIL GUN SIMULATION

1. Notional Railgun Description

Railgun theory was described in Chapter II. The notional railgun used for the simulation model was taken from the Center for Electromechanics (CEM) at the University of Texas. The values assumed for this model include a firing rate of 12 rounds/minute and a projectile muzzle energy of 64 MJ.

2. Pulse Power Supply Simulation Description

The energy storage device simulated in the model for the Railgun and FEL is the flywheel storage system. The system consists of eight flywheels in parallel with each flywheel providing 100 MJ of energy. Figure VI-3 shows the pulse power simulation model in Simulink®. Total stored energy in this system is 800 MJ, which allow a total of

five railgun shots before the energy storage system must be re-charged. The system needs approximately 40 MW from ship's power in order to charge, which takes approximately twenty seconds.

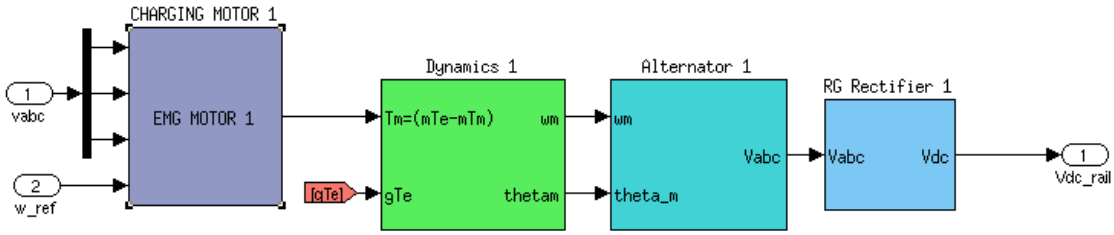

Figure VI-3. Pulse Power Module Built Using SIMULINK®.

C. FREE ELECTRON LASER SIMULATION

The hypothetical FEL used for the simulation environment was chosen to be a 3 MW weapons class laser. The simulation model was built based on three working modes of the FEL, each consuming an estimated amount of power based on the mode of operation.

D. SIMULATION SCENARIOS

Several operational scenarios were simulated using the model.

1. Single FEL Shot

A single FEL shot was conducted with a 5 second duration. Recall, the estimated laser time on target for an engagement to be 5-7 seconds. Figure VI-4 shows the flywheel rotor speed increase to the maximum 18,000 rpm at 12 seconds. The FEL fires at 15 seconds and the rotor loses energy and slows to approximately 17,000 rpm. Figure VI-4, also shows the actual FEL output during the shot. At 14 seconds, the FEL system goes into standby mode in preparation for the shot. In housekeeping mode, only

cooling equipment is expected to be operating. The standby mode is conceived to be the next mode level in which all equipment is operating, minus the actual firing of the FEL. The fire mode is the same as standby, however the laser is in the act of firing. The actual shot occurs at 15 seconds and is five seconds in duration. The FEL consumes an average of 24 MW from the energy storage unit, leaving plenty of energy to conduct more FEL shots or Railgun shots as needed. Multiple shot scenarios and charging of the storage unit between shots will be examined later in this chapter.

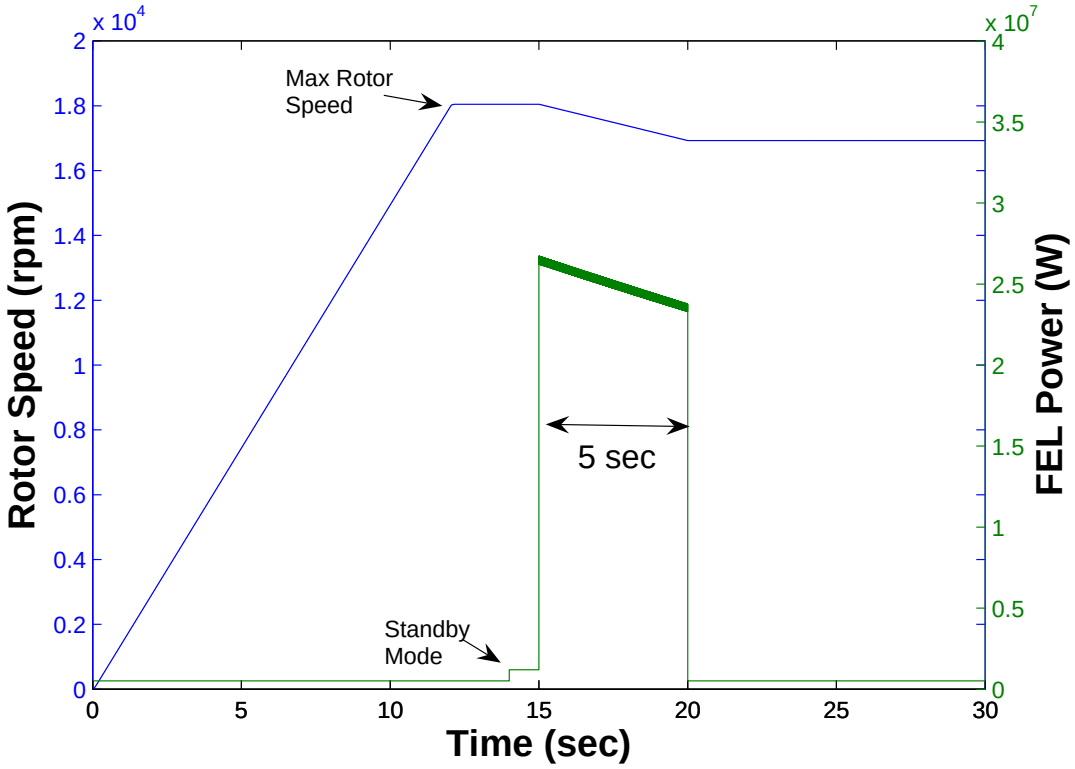

Figure VI-4. Simulation of Single FEL Shot.

2. Single Railgun Shot

A single railgun shot was simulated using a pulse width of 9 ms. Figure VI-5 shows the rotor speed. The

energy storage units are at full energy when the rotor reaches 18,000 rpm. The railgun shot occurs at 14 seconds. The railgun uses up the energy much more quickly than does the FEL, as seen in the figure, the speed drop is almost instantaneous. Figure VI-5 shows the initial stored energy of 800 MJ before the shot and the remaining energy after the shot. The shot consumes approximately 160 MJ leaving 640 MJ for subsequent FEL or railgun shots. This shows that a total of five railgun shots can be conducted on one full charge of the energy storage units. More shots will be shown varying between railgun and FEL shots along with charging of the energy storage unit.

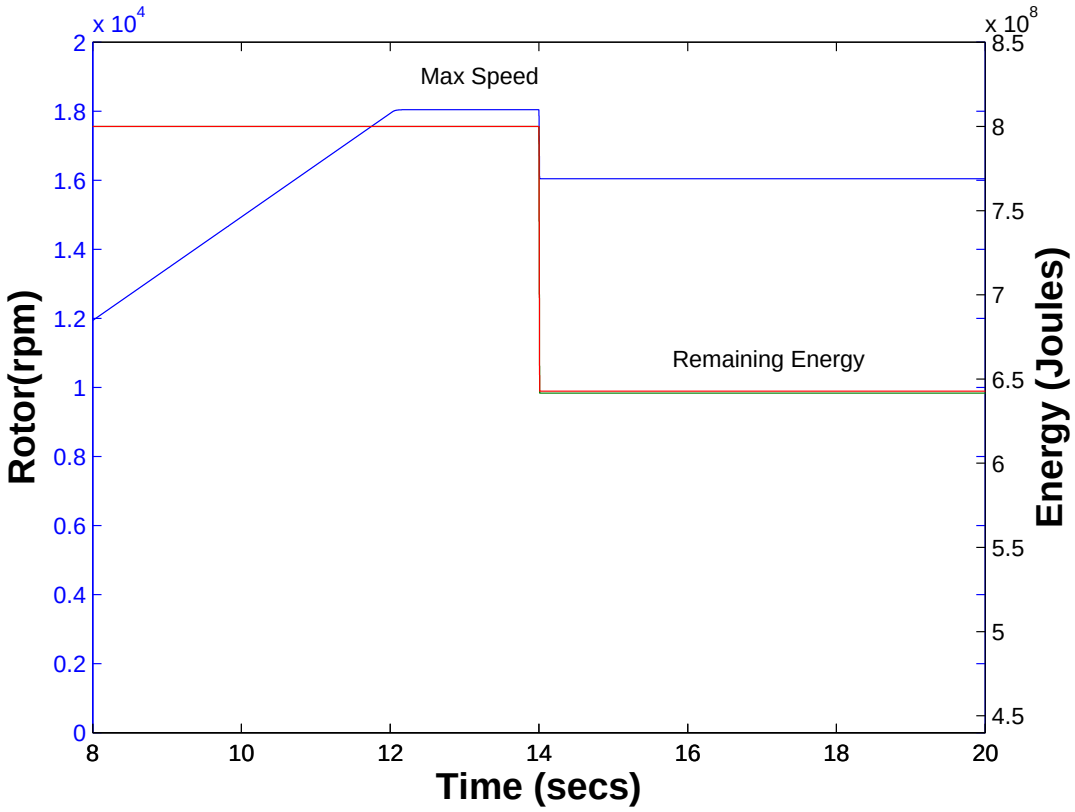

Figure VI-5. Simulation of Single Railgun Shot.

Figure VI-6 shows the power generated by the pulsed alternator (dashed line) and the power consumed by the railgun (solid line). The discharge time for the rail gun is about 9 ms. The power oscillations during the launch are unacceptable in a practical system and can be minimized using a more complex filtering system. The large power spike at launch may be eliminated using an appropriate muzzle shunt [9].

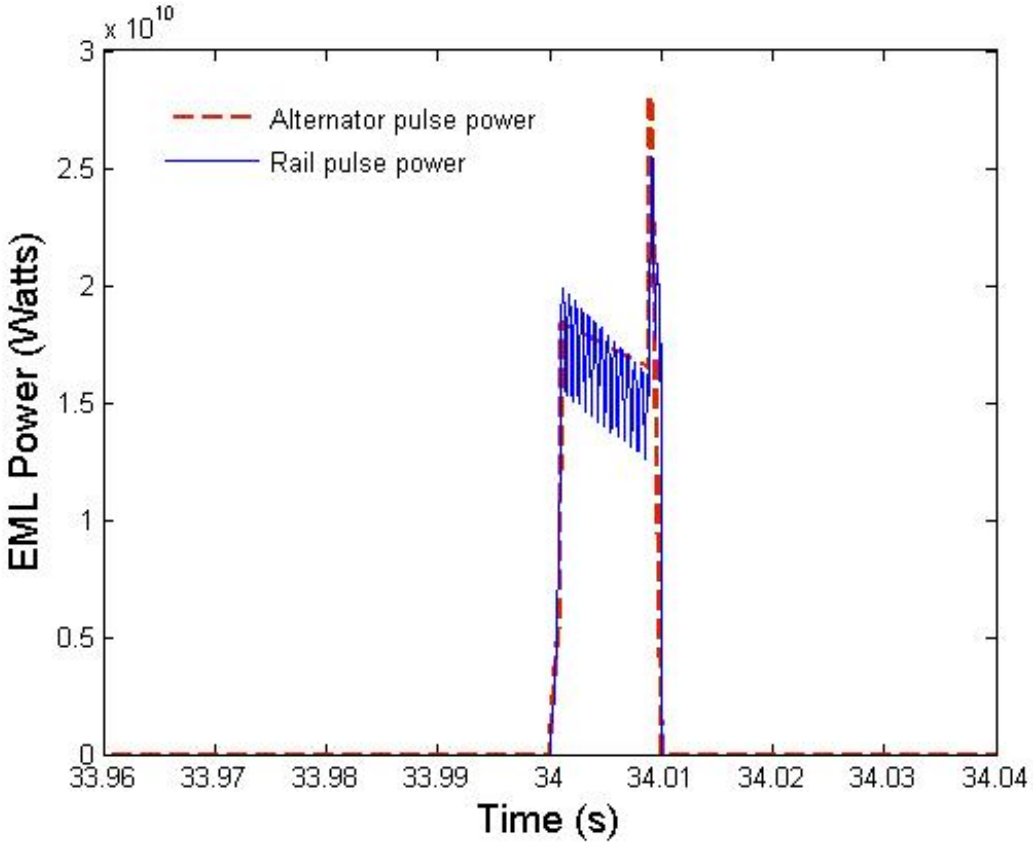

Figure VI-6. Railgun and Alternator Pulse Power. (From: CEM)

3. Four FEL Shots

The next scenario featured a total of four FEL shots using various pulse widths. Figure VI-7 shows the pulse widths very distinctly. The FEL system goes into standby mode at 14 seconds with the first shot fired at 15 seconds.

The first shot is a 5 second pulse width, followed by a 4 second pulse width at 22 seconds. At 29 seconds, a 7 second pulse width shot is taken followed by another 5 second pulse shot.

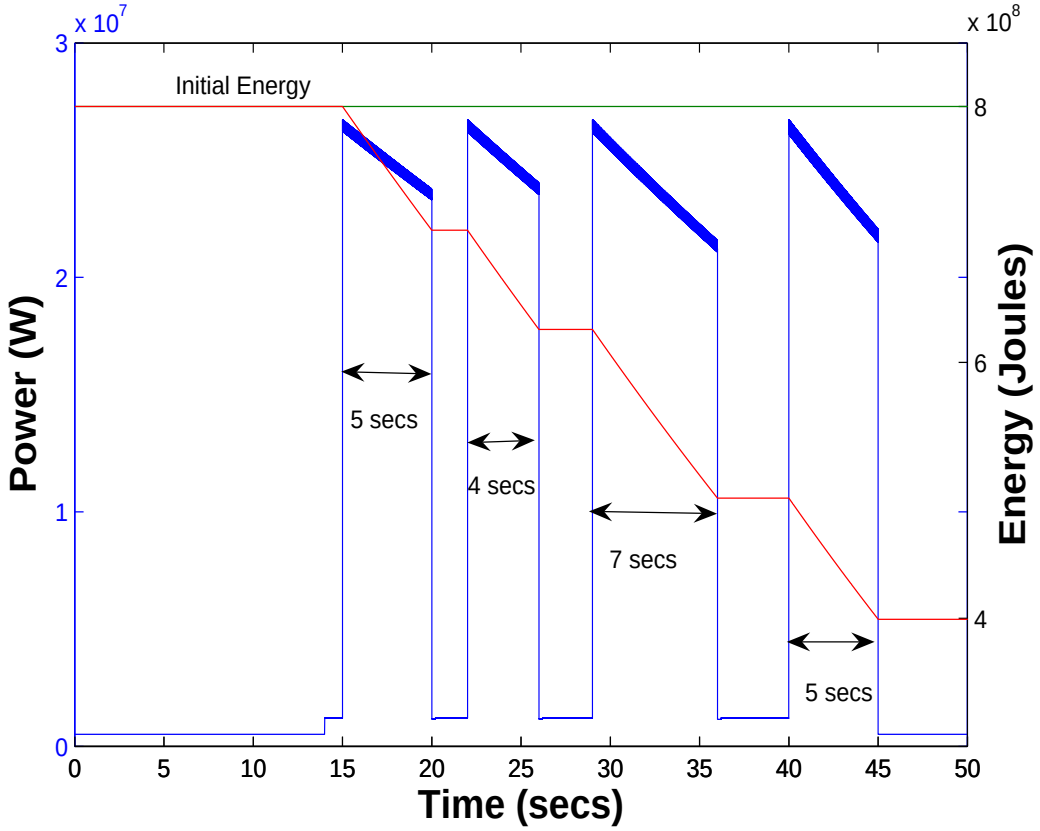

Figure VI-7. Simulation of Multiple FEL Shots.

The energy storage system easily handled the speed and pulse widths of these FEL shots. Figure VI-7 shows the stored energy at 800 MJ prior to the first shot. Each successive shot reduces the available energy accordingly based on the pulse width of the shot. The first shot of 5 seconds consumes approximately 120 MJ. After the completion of the four shots, 400 MJ of energy remains for conducting more FEL shots or railgun shots as needed.

4. Five Railgun Shots

The next scenario uses the energy storage unit to conduct five railgun shots with 9 ms pulse widths. Figure VI-8 shows each of the shots starting with the rotor at maximum speed of 18,000 rpm. The five railgun shots nearly deplete the energy storage unit, so that no further shots can be taken using the energy storage unit. Charging of the energy storage unit must be completed before successive shots can be taken.

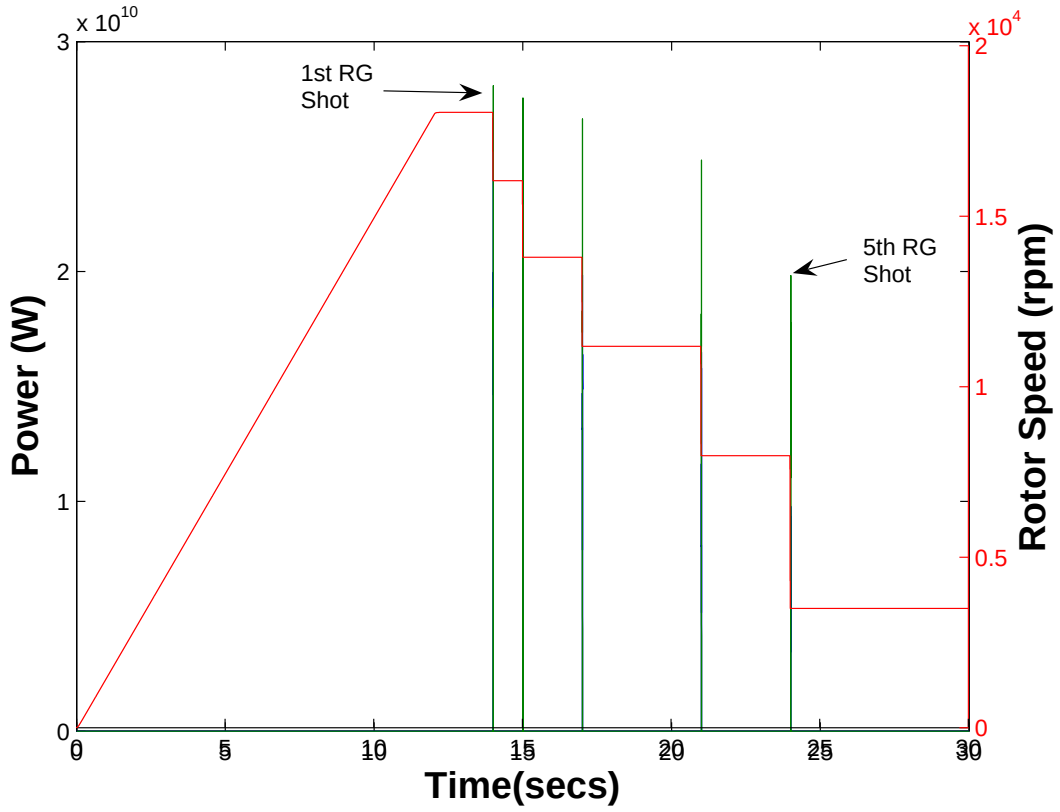

Figure VI-8. Simulation of Multiple Railgun Shots.

5. Two Railgun Shots-One FEL Shot-Two Railgun Shots

The next scenario uses two 9 ms railgun shots, followed by a six second FEL pulse ending with two more 9 ms railgun shots. Again, looking at the rotor data in Figure VI-9, the rotor reaches a maximum speed of 18,000

rpm. The first railgun shot occurs at 14 seconds. After the next railgun shot and the FEL shot at 17 seconds, the rotor speed is reduced to 12,000 rpm. After the next two railgun shots, the rotor speed is down to 4,000 rpm. In Figure VI-9, we see that the remaining energy after all railgun and FEL shots is just under 100 MJ; not enough energy for another railgun shot. However, one more FEL shot can be taken using the energy storage unit.

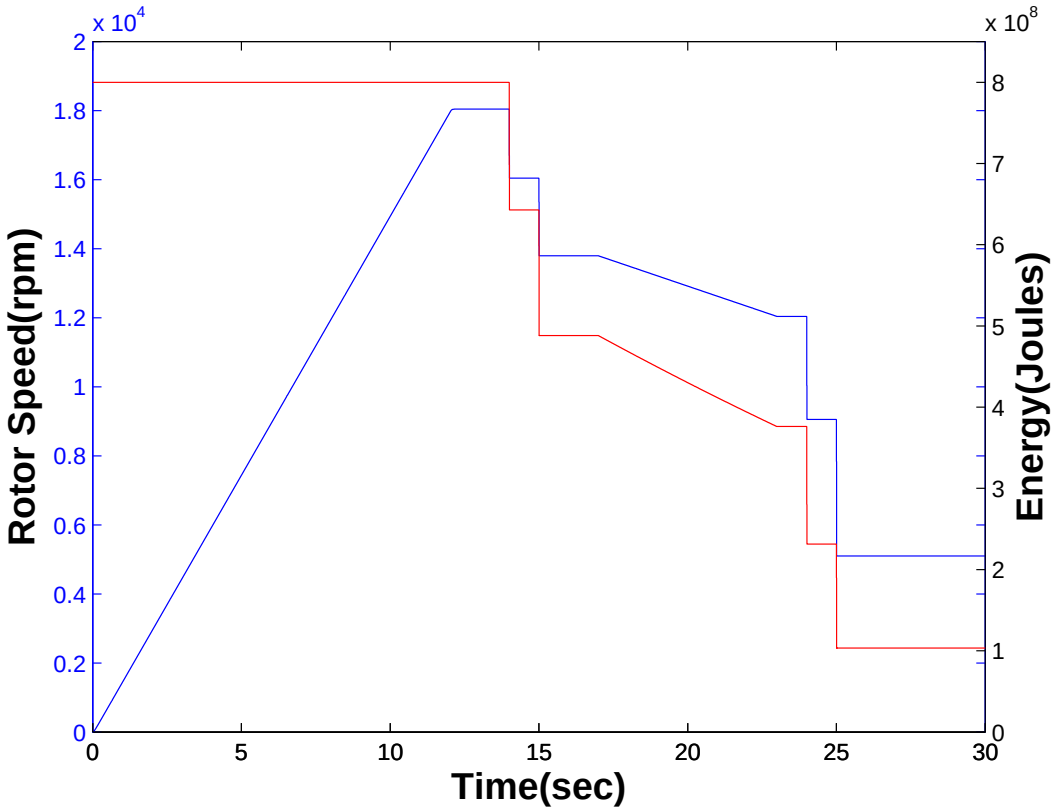

Figure VI-9. Simulation of FEL and Railgun Shots.

6. Four Railgun Shots with Charging

The next scenario involves charging the energy storage device after each railgun shot. Figure VI-10 shows the simulation where again, each railgun shot is 9 ms in duration. The energy storage unit begins at maximum

energy, which corresponds to a maximum rotor speed of 18,000 rpm. After each railgun shot, the rotor takes approximately five seconds to attain maximum speed again. This means that the railgun could be used to support missions hundreds of kilometers inland and still have the energy storage unit fully charged.

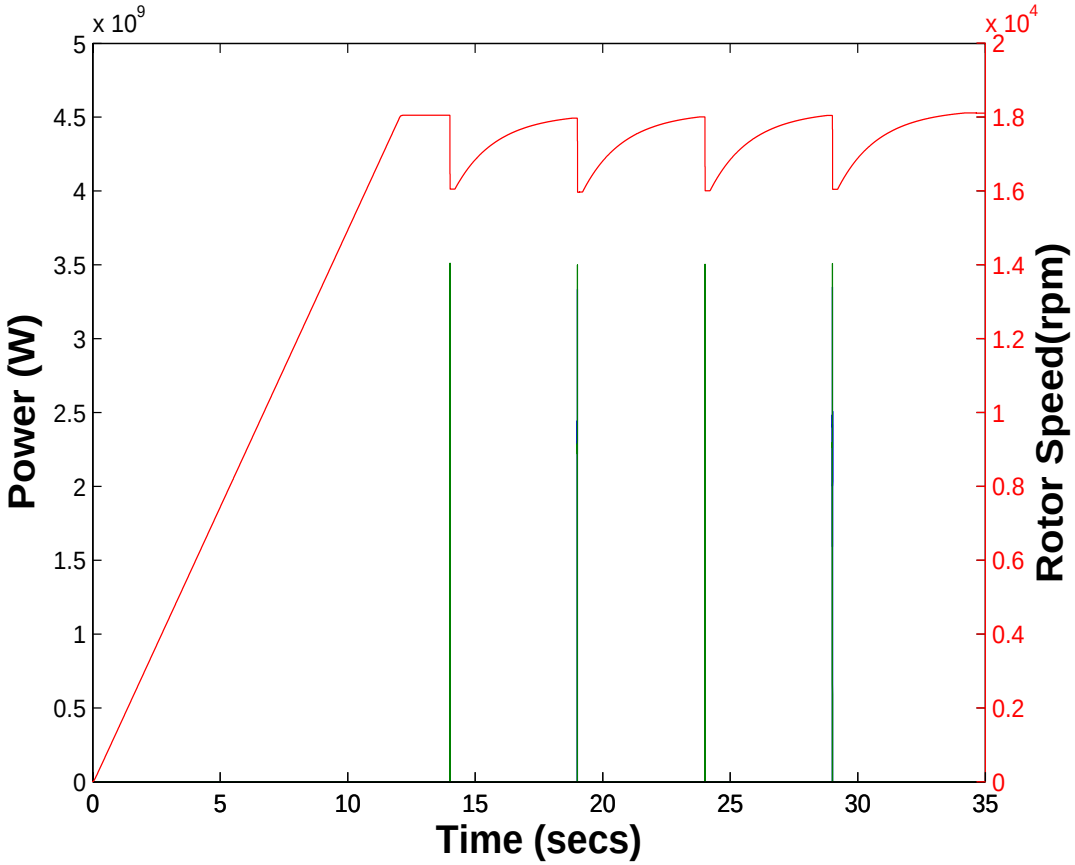

Figure VI-10. Simulation of Four Railgun Shots with Charging.

Figure VI-11 shows the response of the bus voltage to an emergency charge, i.e., all units are connected to the power system simultaneously and charged as rapidly as possible. This simulation suggests that while uncontrolled rapid charging of the system could distort the power grid

for a few cycles, the discharge has no effect. It is likely that the charging effects can be mitigated by better management of power demands [9].

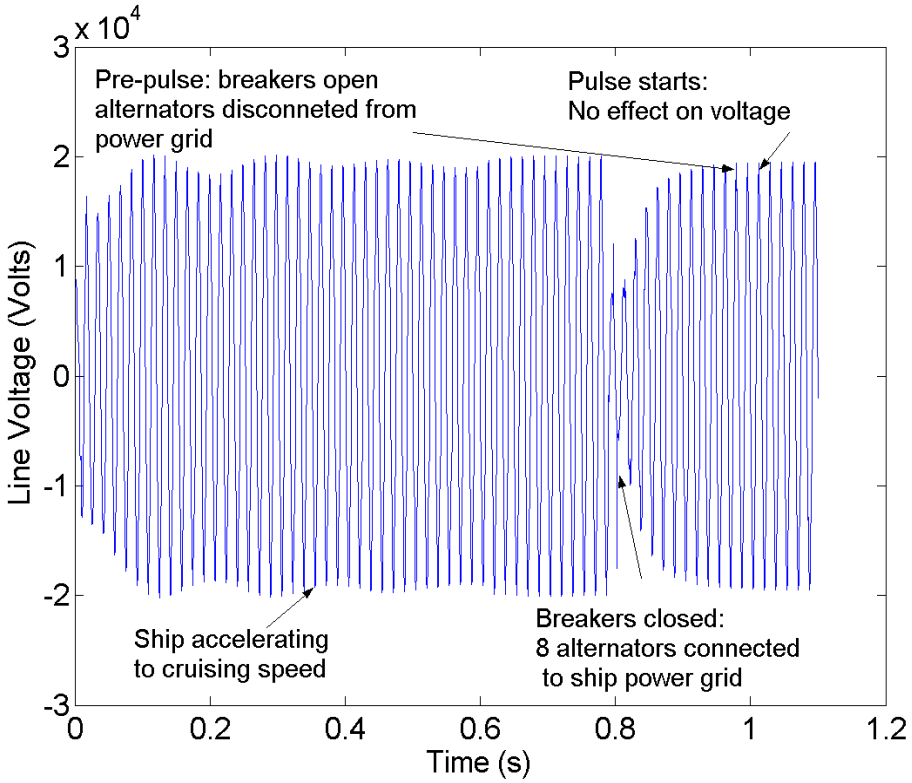

Figure VI-11. Effect on Line Voltage due to Energy Storage. (From: CEM)

7. Propulsion and Electric Weapon Simulation Combined

The last scenario combines the propulsion and weapon simulations to show overall power consumption. Figure VI-12 shows the ship accelerating to a maximum speed of 30 knots. During the speed change, the generators and gas turbines are being held at maximum power. The ship speed is then reduced to 20 knots. At this speed, the energy storage unit is charged. The charging takes approximately 20 seconds while the ship speed is 20 knots. The charging of the energy storage unit would take much longer if the

ship remained at 30 knots. The time to charge is determined by both the available ship grid power and the charging motor rating.

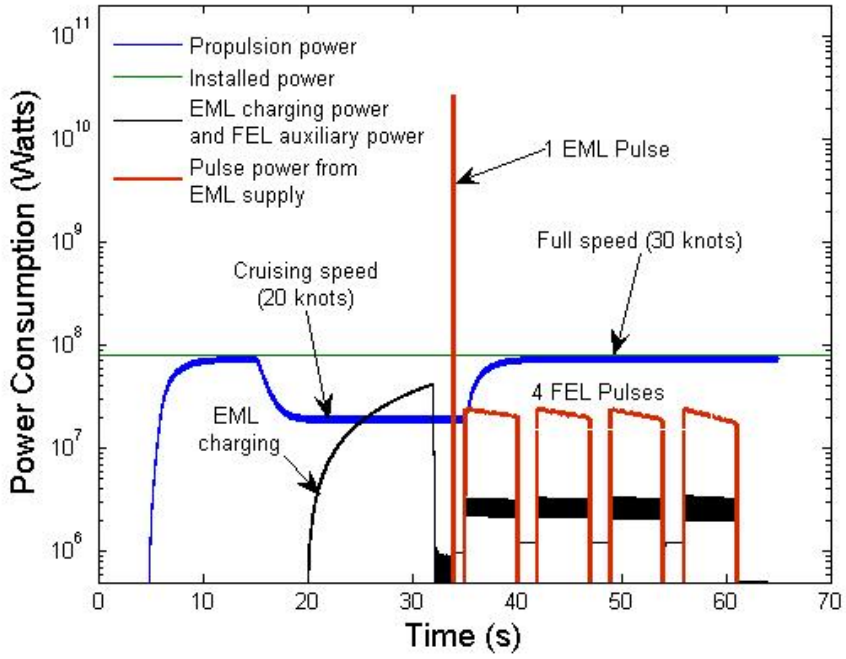

Figure VI-12. Simulation of Propulsion and Electric Weapons. (From: CEM)

THIS PAGE INTENTIONALLY LEFT BLANK

VII. CONCLUSION

High-energy lasers and electromagnetic weapons have the potential to transform the United States Navy to a new level of superiority, giving a tremendous edge over all challenges and adversaries on the high seas. However, many engineering challenges remain, such as integrating these high-powered weapons with the normal ship power grid. A detailed look of the weapon systems effects on the ship's power system is critical in surmounting this obstacle.

An overview of the Free Electron Laser and Railgun has been given along with various methods of potential power sources for these weapons. A hypothetical power system with enough complexity was assumed to allow a good starting point for evaluation of the effects of the electric weapons on the power grid using simulation software. Various scenarios were presented and the results of the simulations were compared.

These simulations show that a railgun and free electron laser can coexist effectively on a future electric ship. These components could share power effectively while allowing enough power to remain available for use as propulsion power. Additionally, these simulations show that the railgun and free electron laser could realistically share the pulsed power energy storage unit.

The simulation used was an effective approach to identifying areas of possible integration issues; however, Simulink® proved to be limited. For example, simulations using both propulsion and weapon shots had to be run separately. A solution to this would be using the lessons

learned in this simulation to write another simulation program using another computer language such as C, which would be better suited to handling the amount of computation.

The new generation of weapons considered for use onboard electric ships promises to change naval warfare, but there is much work still needed to be done before implementation is feasible. While the FEL designs adaptable to a sea environment are ongoing, the railgun is much closer to being realized onboard a ship. The electric ship power system issues must be addressed and solved, but using simulation software such as proposed here. A complete and effective power system can be realized by engineering the power system based on the loads it needs to provide.

LIST OF REFERENCES

[1] Whitman, Edward C., "The IPS Advantage. Electric Drive: A Propulsion System for Tomorrow's Submarine Fleet?" *Seapower Magazine,* July 2001.

[2] Doyle, Timothy J., "An Historical Overview of Navy Electric Drive," *Naval Symposium on Electric Machines,* Newport, RI, 1997.

[3] McCoy, Timothy J., "Trends in Electric Ship Propulsion," *Power Engineering Society Summer Meeting,* Vol. 1, pp. 343-346, IEEE, 2002.

[4] Dudley Knox Library, Naval Postgraduate School.

[5] Trunk, G.V., Hughes II, P.K., Lawrence, J., et al., "Advanced Multifunction RF System (AMRFS) Preliminary Design Considerations," NRL Formal Report 5300—01-9914, December 10, 2001.

[6] Rimmer, R., RE:Slides [Online], RARimmer@jlab.org, 03 January 2006.

[7] W.B. Colson, C. Pelligrini, and A. Renieri. *Free Electron Laser Handbook.* Elsevier Science Publishing Company, Inc., 1990.

[8] Jackson, *Classical Electrodynamics,* 2nd Edition, p. 222, October 1995.

[9] Bowlin, O., Colson, W.B., Domaschk, L.N., Ouroua, A., Hebner, R.E., "Coordination of Large Pulsed Loads on Future Electric Ships," *13th Electromagnetics Launch Technology Symposium,* Berlin, Germany, 2006.

THIS PAGE INTENTIONALLY LEFT BLANK

INITIAL DISTRIBUTION LIST

1. Defense Technical Information Center
   Ft. Belvoir, VA

2. Dudley Knox Library
   Naval Postgraduate School
   Monterey, CA

3. CAPT Roger McGinnis, USN
   Naval Sea Systems Command
   Code SEA 53R
   Washington Navy Yard, DC

4. Prof. James H. Luscombe
   Naval Postgraduate School
   Arlington, VA

5. Prof. William B. Colson,
   Naval Postgraduate School
   Monterey, CA

6. Prof. Robert L. Armstead
   Naval Postgraduate School
   Monterey, CA